Politecnico di Torino

Master of science in Energy and Nuclear Engineering

Academic year 2024-2025

Degree session of November 2025

Techno-economic analysis of hydrogen and carbon-black co-production from thermal pyrolysis of plastic waste

Supervisors:
Prof. Andrea Lanzini
Ing. Giampiero Sacchi

Candidate:
Riccardo Rota

Abstract

Carbon black and hydrogen are two very important commodities in both industrial and energetic fields. Nowadays, they are separately produced from the thermal cracking, distillation, reforming or partial combustion of fossil fuels, with a big environmental impact related to the greenhouse gases emissions of these processes. The co-production of these two materials has been explored in the past by adopting thermal plasma pyrolysis of short hydrocarbons (methane, ethylene), with some good results in pilot plants at industrial scale.

The increasing problems of micro-plastic diffusion all over the world and in every kind of environment is highlighting all the concerns about plastic waste disposal and recycling. Landfilling practices are still very largely used, and the problem of plastic disposal is still far from being solved. For that, possibility of co-producing such precious and useful commodities like hydrogen and carbon black from plastic waste would certainly be a game changer and it is attracting an increasing volume of investments in both scientific and industrial research, which is trying to shift the acquired knowledge in the thermal cracking of hydrocarbons to the thermal cracking of the plastic waste pyrolysis gases.

First of all, an introduction to the different production methods of hydrogen and carbon black is made in order to explain both the most common and the most promising processes, with a focus on the technology readiness level and the production costs. Then, the focus is shifted on the co-production of the two materials, with a technical overview on the more conventional thermal decomposition of methane and on the plastic waste gasification and pyrolysis. The model of a possible industrial process of plastic waste pyrolysis is developed in Aspen Plus, starting from experimental procedures reported in literature. The objective is to assess the potential performances and product yields of the process at full scale and to carry out system optimization and thermal integration to maximize energy efficiency. Finally, a techno-economic analysis is performed, to evaluate the feasibility of the industrial application of the technology. The total energy efficiency of the process ranges to 40% to 48%, depending on the possibility of considering as useful product the heat obtained with the cooling water other than the produced hydrogen and carbon black chemical energy. The obtained hydrogen yield is 6,7g of H_2 per 1 kg of plastic waste, with an hydrogen purity in the final syngas of 94,5%, further processed to obtain pure hydrogen. The final LCOH ranges from 1,75 €/kg to 4,90 €/kg, highlighting the necessity of further research and improvements to make the process suitable for the industrial applications.

List of contents

List of figures

List of tables

Glossary

PAHs   Polycyclic Aromatic Hydrocarbons

SMR   Steam Methane Reforming

CCS   Carbon Capture and Storage

MSW   Municipal Solid Waste

CB   Carbon Black

CNTs   Carbon Nano Tubes

PS   Polystyrene

PE   Polyethylene

PP   Polypropylene

PET   Polyethylene Terephthalate

LDPE   Low Density Polyethylene

WGS   Water Gas Shift

AGR   Acid Gas Removal

PSA   Pressure Swing Adsorption

HER   Hydrogen Evolution Reaction

AWE   Alkaline Water Electrolyser

PEMWE   Proton Exchange Membrane Water Electrolyser

SOEC   Solid Oxide Electrolyser Cell

TRL   Technology Readiness Level

RRCB   Raw Recovered Carbon Black

TPO   Tyre Pyrolysis Oil

TPG   Tyre Pyrolysis Gas

TEM   Transmission Electron Microscopy

NETL   National Energy Technology Laboratory

LCOH   Levelized Cost of Hydrogen

NPV   Net Present Value

BEC   Bare Erected Cost

EPC   Engineering, Procurement, Construction services

EPCC   Engineering, Procurement, Construction Cost

PC   Process Contingencies

PJ   Project Contingencies

TPC   Total Plant Cost

PPC   Pre-Production Cost

INC   Inventory capital

LND   Land cost

FNC   Financing Cost

OOC   Other Owner Cost

TOC   Total Overnight Cost

1. Introduction

Carbon black is a term that includes a large variety of elemental carbon products, such as furnace black, lampblack, channel black and thermal black, that come from thermal treatments of petroleum byproducts. It is a nanostructured material in the form of quasi-spherical particles, generally bonded with covalent links to form aggregates and agglomerates. It can be used as filler in elastomers, plastics and paints in order to change the optical or mechanical properties of the materials in which it is dispersed [1]. With respect to the common soot, it is characterized by a higher surface-to-volume ratio and a very low content of polycyclic aromatic hydrocarbons (PAHs). Carbon black properties depend on synthesis conditions, including feedstock, heating medium, thermal cycles adopted and reactor configuration. Around 70% of the industrially produced carbon black is used as a structural reinforcement in tyres and plastic, especially in the automotive sector. In tyre production it is particularly appreciated for its heat transfer properties, that allow to reduce the thermal damage of the component and increase its durability. This material can also be used for UV radiation absorption and as a pigment in the production of printer ink [2].

Hydrogen is the lightest, smallest and most abundant element in the universe, but it is almost impossible to find it in pure form anywhere. In nature it is bonded with other atoms to form complex molecules, so to obtain pure H_2 is necessary to break the molecule itself. Nowadays, the most common technique to produce it is the steam methane reforming (SMR), that breaks the methane molecule into hydrogen and carbon monoxide. This technology is by far the most convenient in energetic terms, but basically is not carbon neutral unless it is coupled with a carbon capture and storage system (CCS), an expensive and not so widespread technology. A completely on-site emission free process for hydrogen production is water electrolysis, in which the water molecules are split in hydrogen and oxygen. The current technologies employed don't allow to overcome the barrier related to the cost of production, caused almost entirely by the huge amount of energy required to break the bondage between hydrogen and oxygen [3]. Nowadays hydrogen is used in many industrial processes like the synthesis of chemicals, hydrogenation and direct reduction of iron ores for steel production. It is also is considered a very promising energy vector in the pathway to decarbonisation: it can be used directly as a combustible or in fuel cells to decarbonize the transport sector or implemented in the networks in order to partially substitute gas [4].

Novel studies have proved carbon black and hydrogen production from waste to be potentially feasible, even if with some critical points related to the process parameters and

the economic viability. This practice can give multiple benefits in the path towards sustainability. In fact, other than obtaining valuable products and possibly reducing CO_2 emissions by substituting fossil fuels, this practice can prevent thousands of tonnes of waste from landfilling. Waste decomposition in landfills generates methane, which in free atmosphere can contribute to global warming 28 times more than CO_2 over a 100 year time period. Nowadays landfilling is still a widely used practice to get rid of waste, despite the recent progress in recycle processes: in Europe 60 million tonnes of municipal waste are disposed in landfills every year, and this number increases up to 175 million tonnes if also commercial and industrial waste is considered [5].

Both hydrogen and carbon black are valuable commercial products with a very long and important history in industry. Over the decades, many production methods have been adopted and progressively optimized to obtain them in big quantities and at low cost.

In this chapter the most established hydrogen and carbon black production methods, that still largely rely on fossil fuels, will be analysed and compared with the most promising green technologies, that in the majority of the cases are still not mature enough to be implemented at large industrial scale. The development advancement of a technology is described by the TRL (technology readiness level) scale. The scale goes from the values of 1 (only the idea and the basic principles are documented) and 9 (the technology has been developed on large scale and the industrial production has started).

TRL scale	State of technology advancement
1-4	Basic component and working principles are identified
5-7	Development activities and laboratory-scale prototype realization
8-9	Plant scale up and start of industrial production

Table 1 TRL scale and respective technology advancement steps

The different production methods will be therefore compared with each other on the basis of the TRL scale [6].

1.1 Hydrogen and carbon black production

Hydrogen is a very important element in many industrial processes and a promising energy vector for future decarbonization of transport and hard to abate sectors. In particular, it is predicted to be one of the key factors to decarbonize a lot of end uses in the transport and industrial fields. In the automotive sector it could solve many of the typical problems of actual vehicles: larger autonomy is guaranteed, as well as shorter recharge time (refuelling of an hydrogen vehicle could potentially last only a few minutes), while pollutants and greenhouse gases emissions in atmosphere are avoided. In particular, hydrogen vehicles have a more promising future in larger applications, such as trains and trucks. This is because larger vehicles have at disposal more space to host the hydrogen tank, and, as a consequence, lower storage pressure (around 350 bar) is sufficient to store 30-40 kg of H_2, allowing lower pumping cost during refuelling and lower cost of the tank itself. To make possible and convenient the adoption of hydrogen fuel also for automotive applications, where the tank displacement should be limited, very high pressures are required (up to 700 bar) to store just about 6 kg of H_2, making the technical feasibility of the technology a quite challenging point. In the steel production sector, hydrogen is being explored as a reducing agent in the direct reduction iron technique, that allows to produce metallic iron from the reduction of the iron oxide without melting the mineral and so without the need of high temperature heat. In ceramic production, the increment of the gas costs and the big amount of carbon dioxide emissions in atmosphere is leading to an increasing interest in hydrogen as partial substitute of natural gas for combustion, with the creation of mixtures with variable compositions. A similar approach is being used in the glass industry, with the goal of decarbonizing at least the 10% of the overall production process [7].

In 2023 global hydrogen demand was 97 million tonnes, but less than 1% of it was obtained from low greenhouse gases emission technologies, as shown in Figure 1:

Hydrogen production methods
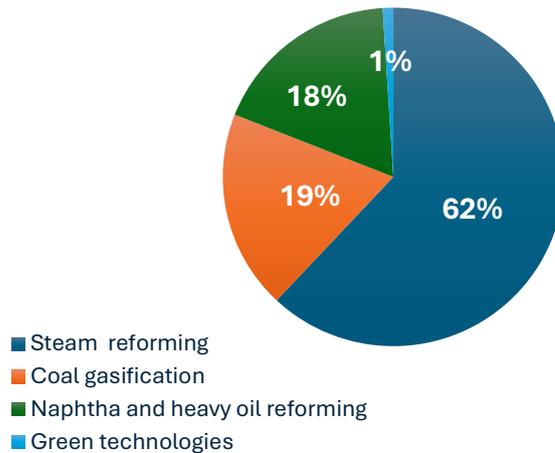
Figure 1 Share of the hydrogen production methods on the total [8]

The main production method is the steam reforming of natural gas, followed by coal gasification and reforming of naphtha and heavy oil.

As a result, the 99% of the hydrogen produced worldwide comes from fossil fuels and the processes adopted are all characterized by high CO_2 emissions [8].

1.1.1 Steam reforming of natural gas

The steam reforming of natural gas consists in the reaction of natural gas with water steam in order to produce hydrogen, carbon monoxide and carbon dioxide. Nowadays it is the most used technology for hydrogen production worldwide and it is commonly coupled with a shift reactor. In order to obtain acceptable reaction rates, a catalyst is required to accelerate the procedure. In this process, half of the hydrogen obtained is originated from the hydrocarbon, the other half from water. The catalyst is a very important process parameter that has to be taken into consideration. Generally, noble metals like Rh, Ru, Pd and Pt are used, but the most common one is Nickel. Ni-based catalysts show good catalytic performance, they are cheap and easily available. However, carbon deposition is one of the main issues in SMR reactors and Ni-based catalysts are particularly sensitive to it: the lower activity with respect to the other noble metals makes it more prone to sintering and coke formation.

14
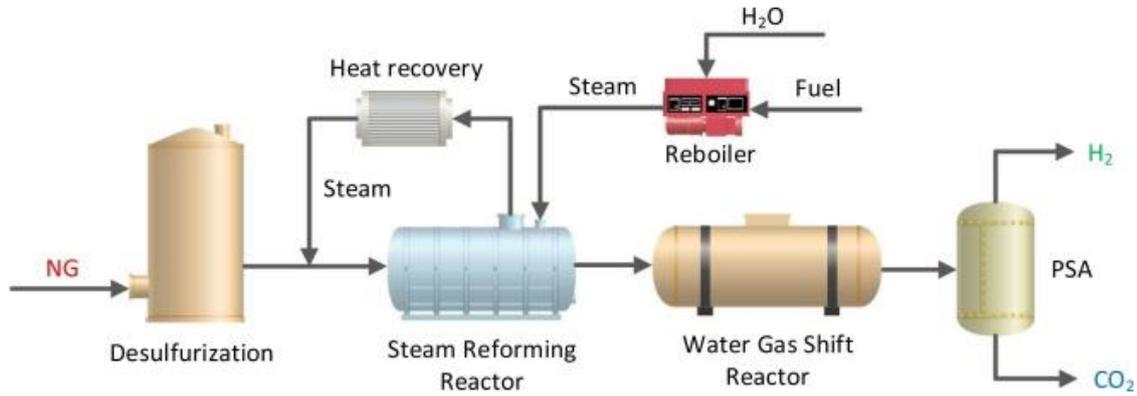
Figure 2 Natural gas steam reforming process [9]

Steam reforming is commonly used for purposes where low hydrogen purity is acceptable, like for the production of methanol or ammonia. The product of steam reforming is a syngas made up by hydrogen and carbon monoxide, so, when the only presence of hydrogen is required, the plant must be coupled with a WGS reactor to convert carbon monoxide in carbon dioxide and hydrogen. The process starts with the purification of the natural gas feedstock. Natural gas is composed almost exclusively of methane, but also heavier hydrocarbons and undesired or dangerous gases, like hydrogen sulphide (H_2S), are included. The natural gas is therefore put in contact in counter-current with a chemical absorber, usually chilled methanol, through the acid gas removal unit (AGR), where desulfurization of the feedstock takes place and the H_2S is removed. The obtained product is then sent into the reformer, where methane and water steam react with steam-to-carbon ratios between 2:1 and 6:1 to give hydrogen, carbon monoxide and carbon dioxide with the following endothermic reactions [9]:

$$CH_4 + H_2O \rightarrow CO + 3H_2 \quad \left(+206\frac{kJ}{mol}\right)$$

$$CH_4 + 2H_2O \rightarrow CO_2 + 4H_2 \quad \left(+160\frac{kJ}{mol}\right)$$
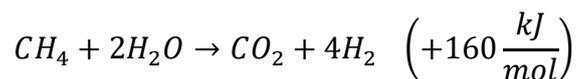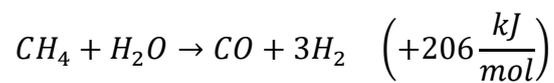
The endothermicity of the reaction raises the necessity of an extra delivery of thermal energy, usually given with the combustion of a fraction of the natural gas that reaches the plant. The reformer systems commercially adopted are made up of tubular reactors crammed with

catalyst pellets and are built in special alloy steels in order to withstand the high temperatures and the reducing conditions. They operate in a temperature range of 700-1000°C and pressure range of 5-35 bar. The obtained syngas is then sent to the WGS reactor, where the exothermic reaction

$$CO + H_2O \rightarrow CO_2 + H_2 \quad \left(-41\frac{kJ}{mol}\right)$$
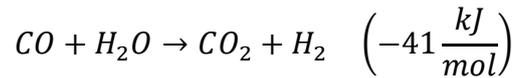
converts the carbon monoxide into hydrogen and carbon dioxide. The final products of the WGS step consists therefore in H_2 and CO_2, so the hydrogen must be separated from the carbon dioxide. The older SMR facilities use amine absorption methods to purify hydrogen, while a more modern solution is represented by pressure swing adsorption (PSA). In amine capture technologies, the absorption of CO_2 is performed by an aqueous solution of various amines (MEA-monoethanolamide; MDEA-methyldiethanolamine; aMDEA-activated methyldiethanolamine), that results in the formation of soluble carbon salts. By heating up the resulting aqueous solution of salts the reaction is reversed and the solvent is regenerated. In cases of presence of syngas with a relatively high CO_2 partial pressure, purification can also be performed with absorption processes based on aqueous solution of calcium carbonate. The process is very similar to the amine absorption methods, but the temperature required is much higher. More modern sorption technologies employed in hydrogen production plants prefer adsorption by porous materials. An alternative method is the pressure swing adsorption, that exploits the possibility of capturing gases at high pressures with different adsorbents. To do that, multiple vessels are used with different purposes: in PSA impurities in the syngas are removed at high partial pressure by using adsorbents and then desorbed at low partial pressure. Then, in the hydrogen separation process from carbon dioxide, the gas with the highest attraction force is trapped, while the other (H_2) passes through the system with a very high degree of purity. There is also the possibility of employing physical processes to remove the carbon dioxide, especially in cases characterized by high CO_2 concentration and low temperature.

These physical processes, like the Selexol or Rectisol ones, can be performed with physical solvents that will periodically undergo regeneration procedures. An alternative to physical

solvents are membrane technologies, where the membrane is permeable only to specific components of the filtered medium. In SMR hydrogen is captured in the membrane and the remaining part of the syngas passes through it. In some cases SMR reactors are designed with an incorporated hydrogen separating membrane. [10]

1.1.2 Coal gasification

Coal gasification is the other most important source of hydrogen production along with SMR. This process turns coal into syngas through several chemical reactions at high temperature and in presence of low amount of oxygen.
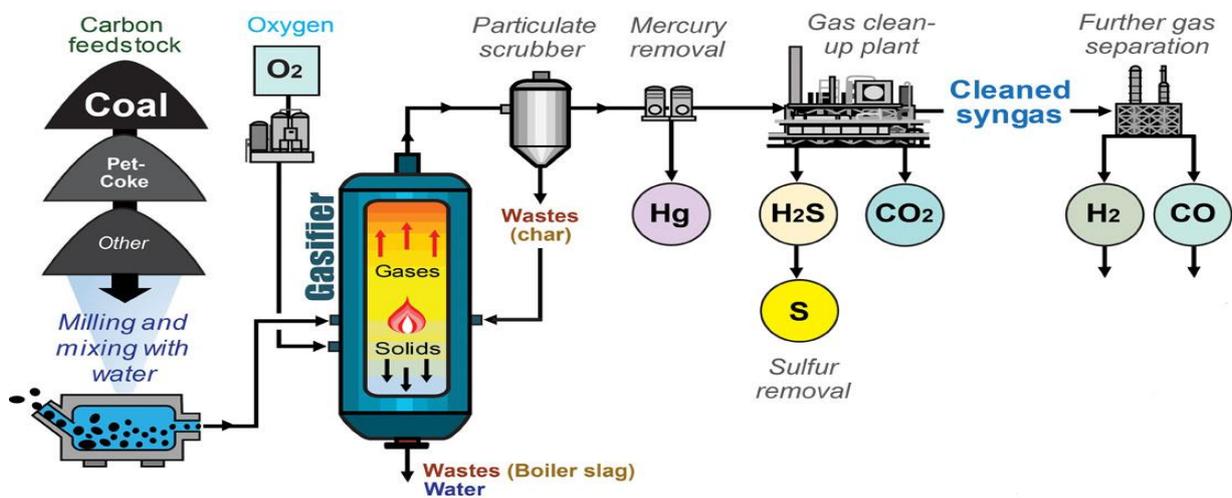
Figure 3 Coal gasification process [12]

The gasification process can be carried out by different gasifier reactors. Not all the gasifiers have the same characteristics in terms of operating conditions, so the main parameters and the several strong and weak points of each one are summarized in Table 2.

Reactor type	Advantages	Disadvantages	Operating parameters
Fixed bed	-High thermal efficiency -Feedstock flexibility -High conversion performance -Low cost	-Low humidity of feedstock is required -More difficult starting and control -High production of char/slag	Temperature: 500-1200°C Pressure: 1-100 bar
Fluidized bed	-Low residue concentration -Good temperature control -Feedstock flexibility -Short residence time	-Size restriction -Requirement of pre-treatment -High investment cost	Temperature: 800-1000°C Pressure: 1-30 bar
Entrained flow bed	-Short residence time -Low residual char -Feedstock flexibility	-Low cold gas efficiency -High cost -Small size	Temperature: 1200-1500°C Pressure: 20-80 bar

Table 2 Reactor types suitable for coal gasification [11]

The coal enters the gasifier in small pieces and reacts with oxygen and water. The reactions between the carbon contained in the coal and the oxygen are the partial oxidation of carbon $\left(C + \frac{1}{2}O_2 \rightarrow CO\right)$, which is the dominant one since the oxygen is injected in under-stoichiometric quantity, and the complete oxidation $(CO + O_2 \rightarrow CO_2)$, both exothermic. The endothermic reaction of water with carbon allows to obtain carbon monoxide and hydrogen $(C + H_2O \rightarrow CO + H_2)$. If the carbon powder is mixed with liquid water to form a slurry before entering the reactor, it will be heated into steam, increasing the reaction endothermicity because of the latent heat of evaporation. Alternatively, water steam can be directly injected in the reactor together with oxygen. The solid and liquid residuals of the gasification processes are evacuated from the bottom of the reactor. The resulting syngas

consists of hydrogen, carbon monoxide and carbon dioxide, along with other undesired gases in very small quantities. After the gasification process, a scrubber cleans the syngas from the particulate particles entrained in the flow. Then, depending on the feedstock quality, variable amounts of mercury particles and hydrogen sulphide have to be removed. Finally, the cleaned syngas can be sent to a shift reactor, where the WGS reaction allows to increase the amount of hydrogen produced. The separation of hydrogen from the carbon dioxide is performed in a CO_2 absorber column that uses chilled methanol as solvent.[12]

1.1.3 Water electrolysis

Water electrolysis is the fourth main method to produce hydrogen, but it contributes to the total production for less than 1%. The main obstacles that prevent water electrolysis from being largely used are mainly related to the high energy demand of the process, since the reaction $H_2O \rightarrow H_2 + \frac{1}{2}O_2$ has a reaction enthalpy of $285\frac{kJ}{mol}$ [13]. This reaction of chemical decomposition of water into hydrogen and oxygen is obtained by externally applying an electric field. In a typical electrolysis cell hydrogen evolves at the cathode, the negative electrode, and oxygen at the anode, the positive one. The efficiency of the process depends mostly on operating pressure and temperature, electrolyte composition and electrode spacing. High temperature improves ionic mobility in the electrolyte, reducing ohmic losses and increasing the current output. Higher cell voltage corresponds to an increase of the electrochemical driving force that boosts the rate of hydrogen formation.

Moreover, increasing ion concentration and reducing electrode distance improves conductivity and minimize internal resistance. There are several different technologies and configurations that allow to obtain water electrolysis. The most established and promising ones are the alkaline water electrolyser (AWE), the proton exchange membrane water electrolyser (PEMWE) and the solid oxide electrolyser cell (SOEC).

AWE is a well established and cost effective technology if compared to the other two, since the technology base is more mature and there is no need of precious metal catalyst. The power capacity of the commercial models is in the order of the hundreds of MW.
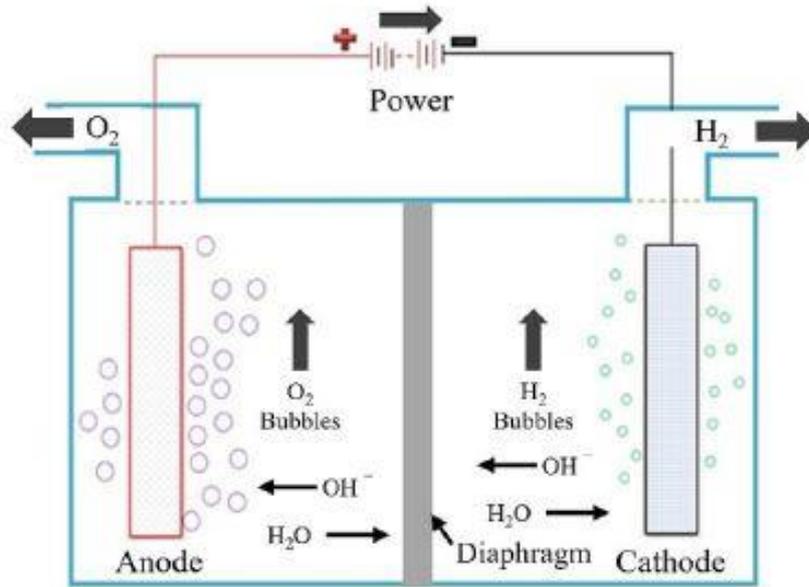
AWE systems typically consist of electrodes immersed into an alkaline aqueous solution and separated by a diaphragm that allows the OH⁻ ion transfer while preventing gas crossover. The semi-reactions at anode and cathode are the following:

$$2OH^- \rightarrow \frac{1}{2}O_2 + H_2O + 2e^- \ (anode) \qquad 2H_2O + 2e^- \rightarrow 2OH^- + H_2 \ (cathode)$$
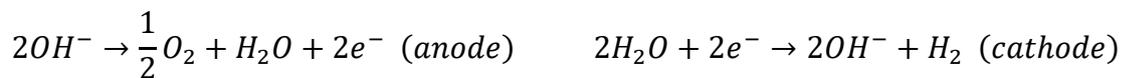
The technology success is related to the low capital cost and the inexpensive membrane that doesn't require the deployment of any noble metal. The main limitations include low current density, formation of carbonate agglomerates and gas impurities. The total energy efficiency of the system is in the range of 70-80%, but further improvements are possible with the optimization of the materials used and the operating parameters.

PEMWE consists in a PEM fuel cell working in reverse. It is one of the most interesting technologies for hydrogen production and is also very promising for future automotive applications. The range of power capacity of commercial models goes from 1kW to tens of MW. With respect to alkaline and solid oxide electrolysers, in PEM electrolysers the charge transfer is performed by the H⁺ ion and the hydrogen is provided at high pressure and low temperature with a very high degree of purity. The key component is the solid polymer electrolyte, commonly in NAFION, that, while enabling proton transport, electrically insulates the electrodes and physically separates hydrogen and oxygen gases. The semi reactions carried out at anode and cathode are the following:

$$H_2O \rightarrow \frac{1}{2}O_2 + 2H^+ + 2e^- \ (anode) \qquad 2H^+ + 2e^- \rightarrow H_2 \ (cathode)$$
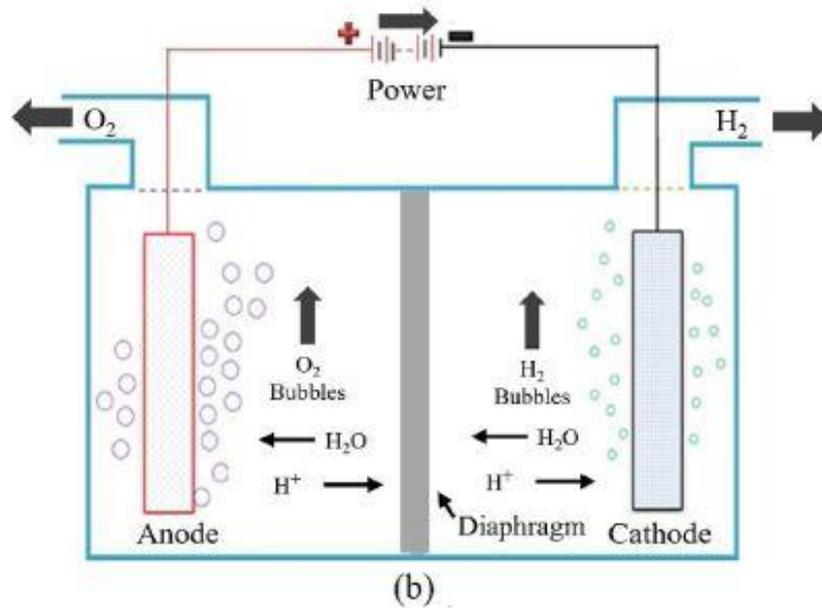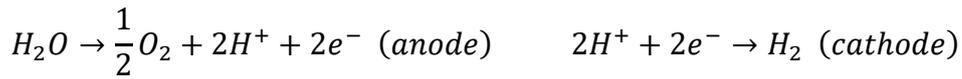
Figure 5 Proton exchange membrane water electrolyser layout [13]

Other than very high hydrogen purity, compared to AWE the PEMWE offers higher ionic conductivity, better dynamic response, smaller system footprint and reduced gas crossover. All these features make possible to reach higher system efficiency (80-90%). However, membrane degradation, catalyst cost and system instability under variable conditions still prevent the technology from being suitable for commercial scalability.

SOEC technology has gained more and more attention as possible solutions for efficient hydrogen production and renewable energy storage due to their high conversion efficiency and their capability to operate at high temperature (typically above 800°C). The developed prototypes have a power capacity that can go from 1 kW to 200 kW. SOECs convert electrical energy into chemical energy by electrolyzing steam in pure hydrogen and oxygen, with the charge transfer carried out by the O^{2-} ions, with the following semi-reactions at anode and cathode:

$$O^{2-} \rightarrow \frac{1}{2}O_2 + 2e^- (anode) \qquad H_2O + 2e^- \rightarrow O^{2-} + H_2 (cathode)$$

SOECs are characterized by extremely high efficiency (90-100%) when operating high temperature steam electrolysis, but the system still exhibits excessive degradation rates when used in electrolysis mode [14].
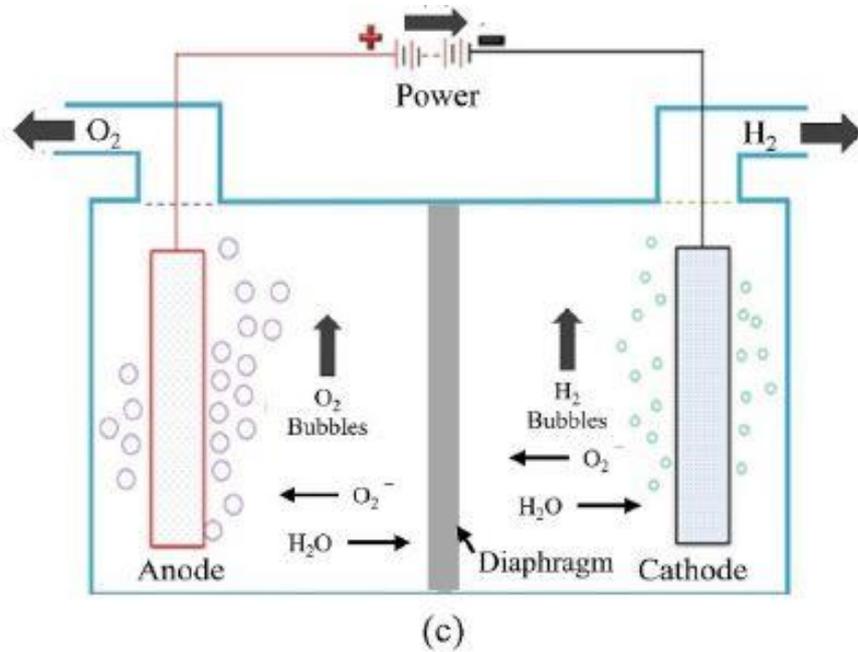
Figure 6 Solid oxide electrolyser layout [13]

1.1.4 Biomass gasification

Biomass gasification is a thermochemical process carried out in a range of temperature between 500 and 1400°C that breaks down the feedstock into tar, char and hydrogen rich syngas. Depending on the element used as oxidizing agent, the process can be classified as air, oxygen or steam gasification. This last one is the most common [15]. Generally speaking, industrial gasification processes are all characterized by the same stages. A common plant configuration is shown in Figure 9.
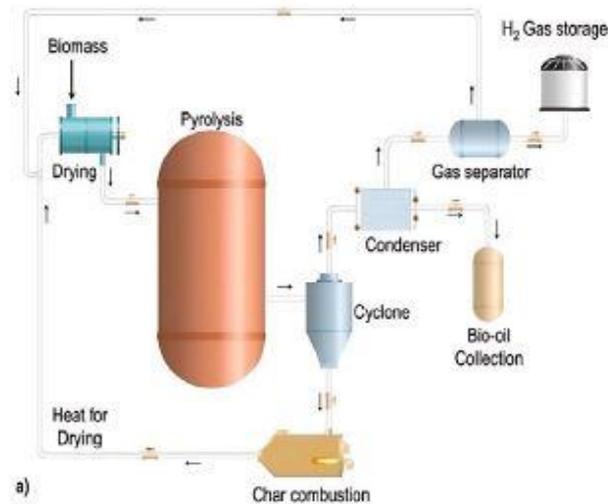
Figure 7 Biomass steam gasification process [9]

The typical biomass used for gasification purposes has a moisture content of 5-35%, so a drying process at a temperature of 150-200°C is required in order to take this amount at values lower than 5%. Then, in the pyrolysis reactor the thermal decomposition of the feedstock in absence of oxygen takes place, with the release of hydrocarbon gases and the conversion of biomass in solid charcoal. With the introduction of sub stoichiometric oxygen in the reactor, the oxidation of the carbon and hydrogen still present in the solid fraction of the biomass takes place, giving CO, water and a large amount of heat as product. Then, at a temperature of 800-1000°C a series of endothermic reduction reactions contribute to the formation of the final syngas:

$$Water-gas\ reaction\quad C + H_2O \rightarrow CO + H_2 \quad \left(-131\ \frac{kJ}{mol}\right)$$

$$Bounded\ reaction\quad C + CO_2 \rightarrow 2CO \quad \left(-172{,}6\ \frac{kJ}{mol}\right)$$

$$Shift\ reaction\quad CO_2 + H_2 \rightarrow CO + H_2O \quad \left(-42\ \frac{kJ}{mol}\right)$$

$$Methane\ reaction\quad C + 2H_2 \rightarrow CH_4 \quad \left(75\ \frac{kJ}{mol}\right)$$
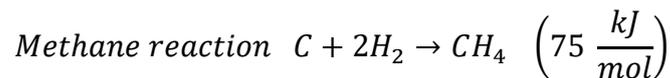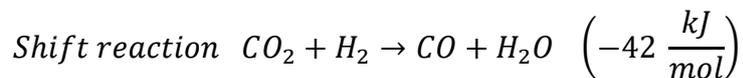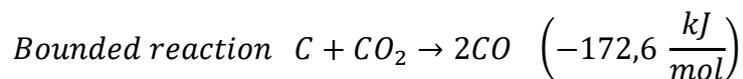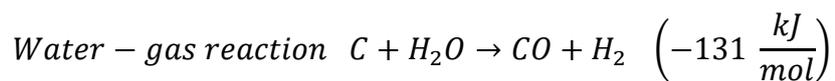
The obtained solid and gaseous products are sent to a cyclone separator, where the char is separated from the syngas. In order to increase the efficiency of the system, the heat needed for the drying stage can be obtained from char combustion. The syngas is passed through a

condenser where the heavier hydrocarbons precipitate to form useful bio-oil, while the light fraction is sent to a gas separator in order to obtain the hydrogen [16].

1.1.5 TRL and costs comparison

As said at the beginning of the chapter, 99% of the hydrogen production is covered by methods that use fossil fuels as feedstock. As a consequence, even if hydrogen is considered one of the most promising energy vectors for decarbonization, its sustainability is still affected by the big amount of greenhouse gases emissions during the production process. However, those traditional methods are still by far the cheapest way to obtain hydrogen and make economically sustainable its adoption at large industrial level.

Technology	Hydrogen cost ($/kg)	TRL
NG reforming	1,2-2,4 [17]	9
Coal gasification	1,9-2,4 [18]	9
Naphta reforming	1,6 [19]	9
Water electrolysis	5,2-13,2 [17]	6-9
Biomass gasification	1,7-4,1 [17]	7-9

Table 3 Hydrogen cost and TRL of the different hydrogen production methods

Natural gas reforming is the most established technology and allows to produce the cheapest hydrogen. The long industrial history of this production method makes his technologic development almost static, with no significant improvement reported in the last years. The same could be said for coal gasification and naphtha reforming, that both allow to produce very cheap hydrogen.

For what concerns the most innovative methods, water electrolysis and biomass gasification, the analysis is a bit more complex. Water electrolysis can produce hydrogen with a very variable cost, depending on the electrolyser technology and the energy source adopted. Moreover, not all the electrolyser technologies have the same TRL. Alkaline electrolysers are the most developed in terms of technology readiness (TRL 9) and allow to produce relatively cheap hydrogen compared to the other technologies.

AWEs that use electricity from wind resources produce hydrogen at around 9$/kg, going down to 8$/kg in the case of the adoption of solar PV as electricity source. PEMWE have

also been proven to be a valid alternative for industrial hydrogen production, even if their large scale industrial deployment still has to start (TRL 8). The high degree of purity of the hydrogen produced with this technology makes it very interesting for the future, but nowadays this also represents the most expensive production method (9$/kg with wind energy source, 13$/kg with solar PV energy source). SOEC represents also a very promising pathway for hydrogen production, with very fast technologic improvements. Nowadays it is still considered an experimental technology (TRL 6-7). Interestingly, SOEC prototypes fed by electricity coming from solar PV resources have been able to produce hydrogen at around 5$/kg, potentially making it the cheapest electrolyser technology.

Biomass gasification is another innovative technology that allows to produce hydrogen from renewable sources. The cost of hydrogen production is relatively low and comparable to the more traditional methods using fossil fuels. This peculiarity is related to the gasification process adopted, which is quite similar to the one of coal. However, this solution is still limited to a few production plants all over the world

1.2 Carbon black production methods

Carbon black is a material made up by elemental carbon and traces of nitrogen, sulphur and oxygen, arranged in colloidal particles of different sizes. The most important properties of carbon black are the structure, the surface area and the primary particle size. The primary particle is smallest unit of a CB particle, that can form aggregates of different sizes. Size, shape and void volume in the carbon black aggregate determine the end use of the product.

The overall, carbon black production worldwide reached 14 million tonnes in 2024. The biggest carbon black producer in the world is the Indian company Birla Carbon, that produces alone 2 million tonnes annually. Other important companies like Continental Carbon Company and Orion S.A are American, indeed, United States is the most important country in terms of carbon black production [20]. Around 90% of the total produced CB is employed in the tyre industry, 9% is used as pigment in the paint industry and the remaining 1% is employed as innovative material in the electricity field to improve cable insulation and battery energy storage efficiency [21]. In particular, in the tyre industry carbon black is used as a tyre filler in order to improve the heat transfer in the most sensitive hotspots, like the groove and the belt. As a result, the thermal stress on the tyre is reduced and the longevity

increased. Carbon black is also largely adopted as a pigment in paints and high performance coatings, improving thermal conductivity and protection from UV radiation degradation. Thanks to the very good electrical properties, CB is also used in the production of cables for conductor insulation. Other applications in promising sectors and technology include the use of CB in batteries to improve the electrochemical conductivity, the charging performance and the overall efficiency of the system.

Carbon black is commonly produced by either incomplete combustion or thermal decomposition of gaseous or liquid hydrocarbon-based feedstock. Historically furnace, thermal, acetylene and channel methods have been adopted for the production. Nowadays, the furnace process has substituted almost entirely all the mentioned production methods, accounting for more than 90% of the total CB production. The remaining part is almost completely covered with the thermal method [22].

1.2.1 Furnace black

The furnace process uses heavy aromatic oils taken from low cut fractions of previous refining processes as feedstock. The production furnace uses a closed reactor to firstly atomize the feedstock oil under controlled temperature conditions and to eliminate non-carbonaceous materials. Then, the obtained product is sent to the reactor where it is combusted in controlled atmosphere and at temperatures between 800°C and 1200°C. Oxygen levels are continuously controlled and kept under the critical value that would enhance undesired soot formation. In this phase, the carbon atoms begin to bond within the feedstock droplet, building up the primary particle, the fundamental carbon black particle. As the carbonizing fuel droplet leaves the reactor, the formed primary particles come in contact with each other and start to form carbon black aggregates. The reaction can be quenched by temperature control and water addition, in order to modify chemistry, size and complexity of the aggregates. After the quenching and the heat exchange carried out in the oil pre-heater, the separation of the carbon black from the gas stream finally performed into bag filters or cyclone separators. At this point, the obtained CB is referred as 'fluffy' and is characterized by very low bulk density. Therefore, if further densification is required, vacuum rollers, pin pelletizers and stirred tanks can be employed at the end of the process. The mixture is then sent to a drier where the volatile matter is evaporated and the dried

carbon black is finally sent to the drum magnet where it is separated from rust and iron particles [23].
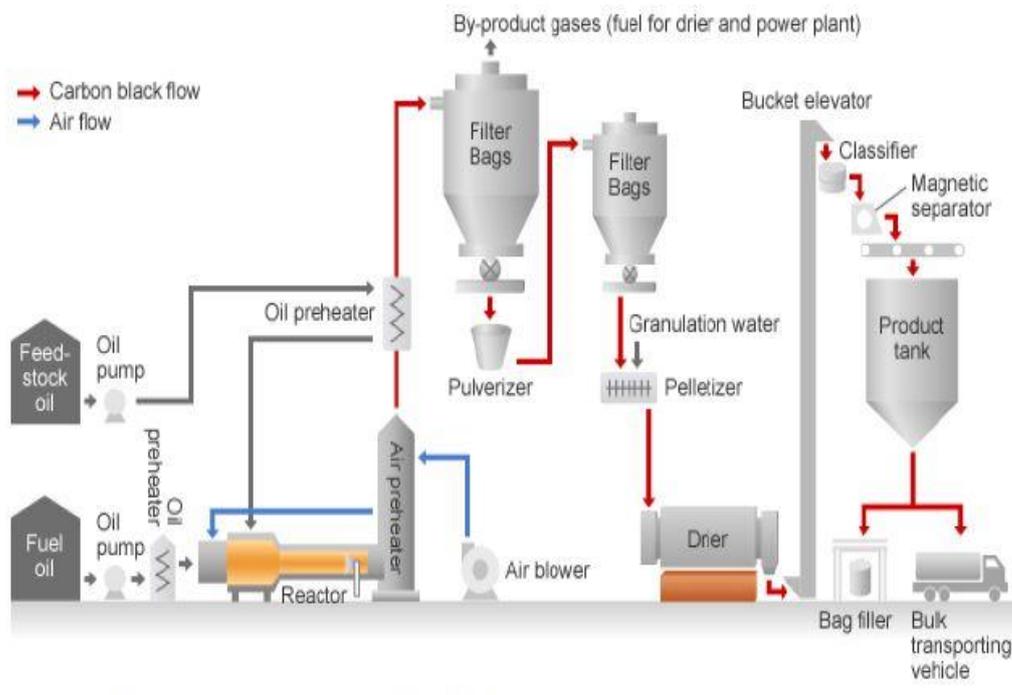
Figure 8 Furnace black production process [24]

1.2.2 Thermal black

The thermal black process uses primarily methane and heavy aromatic oils as feedstock. In the process a couple of furnaces alternate every five minutes approximately between pre-heating and carbon black production. The natural gas is injected into the inert atmosphere of the hot refractory lined furnace where it decomposes into carbon black and hydrogen-rich syngas. The aerosol material is then quenched with water sprays and collected in a bag filter. The obtained carbon black can be further processed for impurities removal or pelletization. Once the CB is processed and reaches the desired quality is finally screened and packed for shipment. The resulting syngas is used internally to the plant in order to be burnt in air and preheat the second furnace. An alternative feedstock commonly adopted in the thermal process is acetylene, with the obtained carbon black named acetylene black.

Typically, the thermal black is characterized by larger primary particle size but, at the same time, a very low degree of particle aggregation. Given the possibility of using natural gas as feedstock, it also gives the possibility to obtain one of the purest forms of carbon available on the market [22].
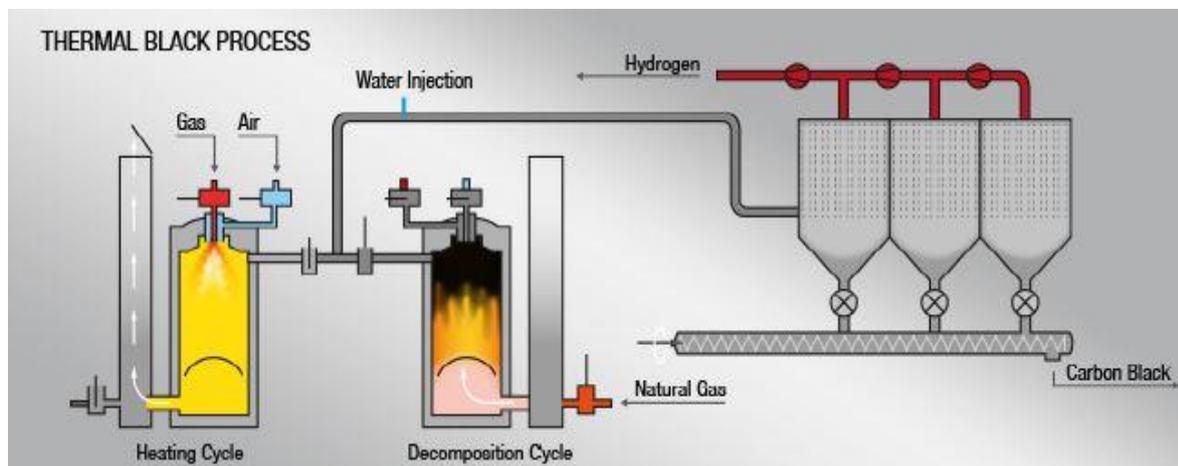
Figure 9 Thermal black production process[25]

1.2.3 Channel black

The channel method is another traditional method to produce carbon black. Nowadays is almost not adopted anymore because of the substitution of this production process with the furnace method. With respect to the furnace method, the channel process is characterized by higher amount of oxygen supplied for the partial combustion and lower combustion temperature (approximately 500°C). Moreover, given the elongated shape of the typical channel black plant, the residence time of the feedstock into the reactor is longer, in the order of a few seconds. Usually, channel black undergoes an aftertreatment process with oxygen, always at 500°C [24]. This passage the surface becomes oxidized and oxygen-containing functional groups are added. With respect to the commercial furnace and thermal blacks, channel black is characterized by lower degree of aggregation, larger specific surface area and finer particle size, making it suitable for food-contact carbon black. Moreover, thanks to the oxygen-containing functional groups is also employed to slow down the rubber vulcanization and to improve the printing properties of ink [25].

The channel black production process is shown in Figure 10.

28
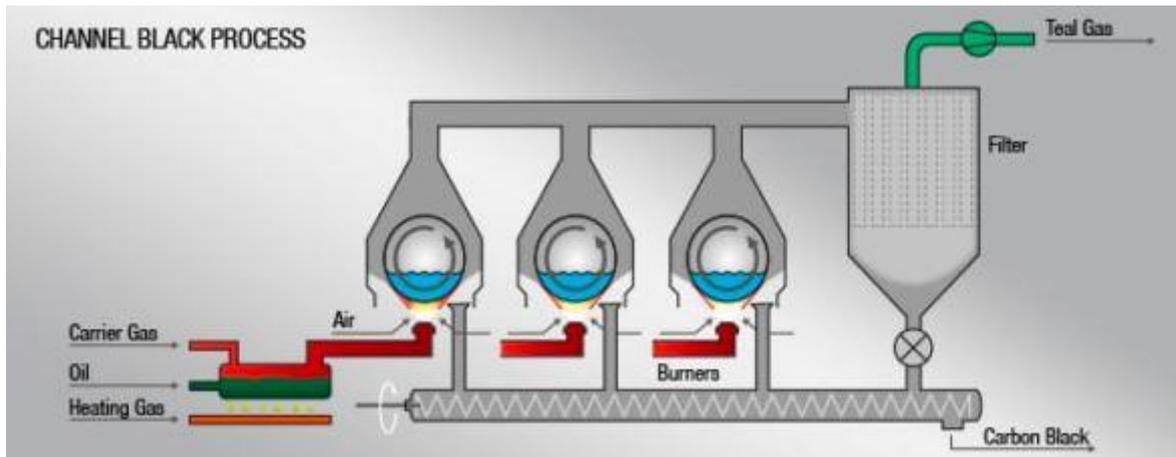
Figure 10 Channel black process [25]

1.2.4 Waste tyre pyrolysis

The most promising innovative production process of carbon black uses the spent tyre pyrolysis. This method is considered to be particularly interesting because makes the carbon black production independent from the price fluctuations of fossil fuels. This is a crucial point, because the feedstock is estimated to account for the 60% of the total manufacturing cost. This technology also represents a first attempt to obtain carbon black from some kind of waste, improving the environmental performance with respect to the conventional process. Generally, the waste tyre pyrolysis is carried out at relatively low temperatures (450-600°C), with rapid water quenching. The pyrolysis reactors most adopted for this purpose are the auger reactor and the moving bed reactor. In order to make the process more economically sustainable, carbon black production is coupled with tyre pyrolysis oil (TPO), which can be further converted in valuable fuel [26].

A very important pilot plant, revamped and tested many times over the years, is located at the Instituto de Carboquimica in Zaragoza. Its working principle represents the starting point of the semi-industrial plants located all over the world. The spent tyre pieces are fed by means of an agitated hopper. The heat required for the pyrolysis is obtained with three electrical resistances put on the reactor walls. There are two reactor outlets, one for the solid char and one for the pyrolysis gases to be condensed later.

Nitrogen is also injected at the bottom of the reactor in order to minimize air intrusions and keep the inert atmosphere. It has been experimentally proved that N_2 injection doesn't affect the volatile residence time. The pyrolysis gases leave the reactor and reach the condenser, where the liquid and gaseous fractions of the product are separated. The char collected at the bottom of the pyrolysis reactor contains a very high yield of carbon black, along with traces of iron and other metals. The semi-industrial plant based on this technology is located at the Parque tecnologico de reciclado in Zaragoza and its layout is shown in Figure 11.
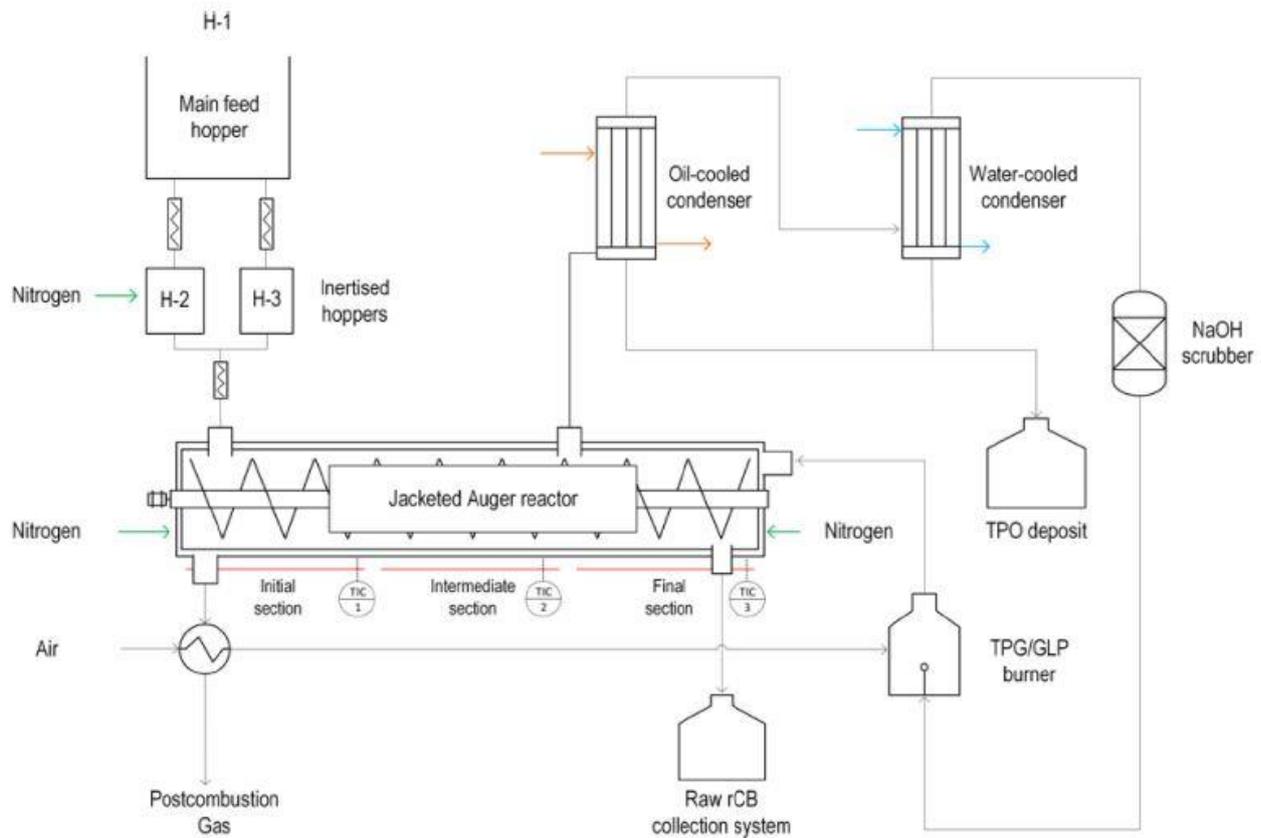
Figure 11 Semi industrial prototype of waste tyre pyrolysis plant with auger reactor [29]

The plant is able to elaborate 400 kg/h of waste tyres and is based on the auger technology using the results and operational features of the pilot plant previously described, even if some differences are present. The hoppers are sealed and inserted under nitrogen atmosphere. The configuration with the two hoppers aims to obtain a continuous operation while one of the two is filled. The heating of the reactor is provided by the combustion of the tyre pyrolysis gas (TPG) and supported by an auxiliary gas burner. Moreover, the resulting flue gases are provided to a counter current heater to heat up the feedstock at the reactor inlet [27].

Another interesting example of a plant developed on industrial scale for the waste tyre pyrolysis is located Dillingen/Saar and is managed by the company Pyrum Innovations AG. The goal of the company is to contribute to the oil and gas sector decarbonization by introducing on the market valuable and usable waste tyre pyrolysis oil. The solid byproduct of this process is RRCB (Raw Recovered Carbon Black), which shows very similar physical properties with respect to the conventional furnace black. The layout of the plant is very similar to the one previously presented, with the main difference consisting in the reactor technology.
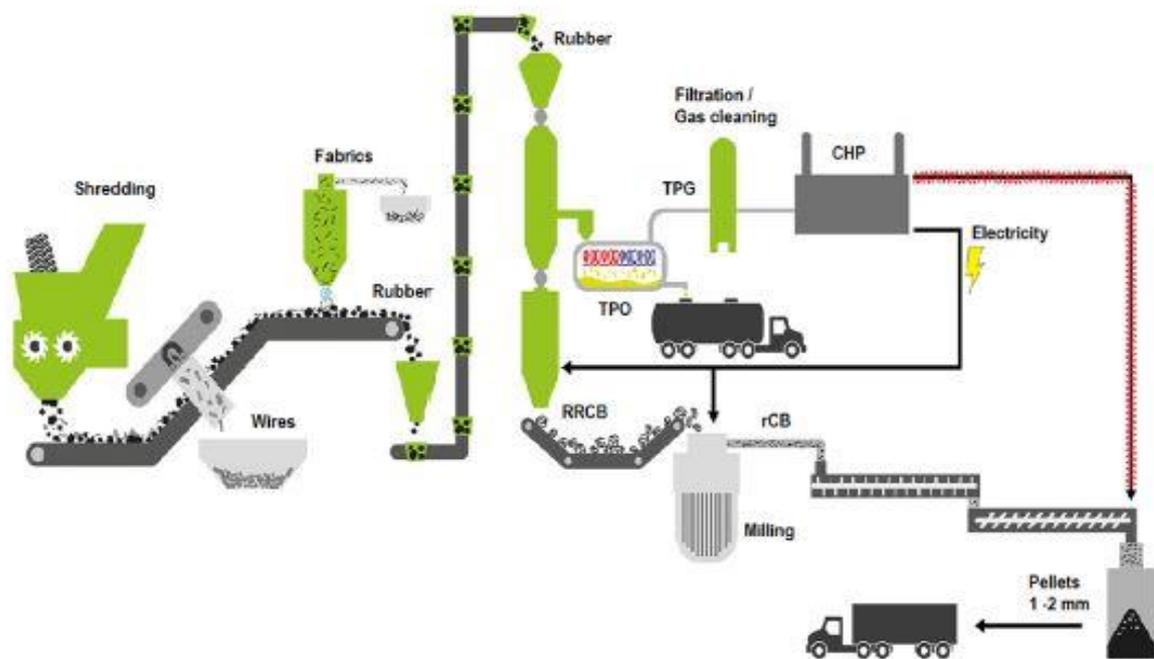
Figure 12 Industrial waste tyre pyrolysis with a moving bed reactor [30]

The plant consists again of three different systems: the pyrolysis reactor, the condenser and the RRCB collection. The plant is able to process up to 5000 tonnes of feedstock per year. The tyre is firstly shredded and the wire and fabric materials are separated by magnetic and pneumatic systems, then the rubber feedstock is delivered with granules size lower than 8 mm. The pyrolysis is carried out in a vertical cylindrical moving bed reactor, electrically heated at a temperature range of 500-750°C. The process delivers 35% TPO, 45% RRCB and 20% TPG. The residence time of the rubber granules into the reactor is determined by the dosing devices installed, but is always longer than one hour. The condensation unit receives the pyrolysis gases and separates TPO from TPG. TPG is sent to a combined heat

and power unit after being filtered and purified, in order to generate the electricity needed to power both the pyrolysis reactor and the RRCB mill. The RRCB is continuously extracted from the bottom of the reactor via sluice systems and then sent to the pelletizing units [28].

In recent years, also the direct adoption of tyre pyrolysis oil as feedstock for the conventional furnace process has been investigated, and more and more companies are getting involved in the testing of the process. In February 2025, Orion S.A., the fourth biggest company in the carbon black production sector, started a partnership with Contec S.A. to source TPO for circular carbon black production. Hankook Tire and Technology, one of the biggest tyre producers in the world, started a consortium with 12 partners in South Korea to experiment the production of tyres using carbon black from TPO [20].

1.2.5 TRL and cost comparison

As seen at the beginning of the chapter, the carbon black production is almost entirely covered by the furnace and thermal processes. Between these two old and established technologies (TRL 9) there is no particular difference in the production costs, varying between 1,6 and 1,75 $/kg depending on the cost of energy and feedstock of the specific location. Channel black is an even older technology, which has almost disappeared since the lighter and smaller particles that produces are now obtainable also with the furnace technique.

Technology	CB cost ($/kg)	TRL
Furnace process	1,6 [29]	9
Thermal process	1,7 [29]	9
Waste tyre pyrolysis	0,8-1 [19]	7-8

Table 4 Carbon black cost and TRL of the different hydrogen production methods

The possibility of using a waste material whose end of life disposal is considered a critical point and of a strong reduction in the pollutant emissions of the carbon black production process is represented by the waste tyre pyrolysis. Plethora of studies about this concept have been conducted since the first 2000s resulting in the first semi-industrial plant prototypes in the last few years. This phase of technology development is the most critical, since it is exactly the point in which usually there is no more the economic help of public or academic institutions and is up to the private investors to put the money in innovative concepts that

are still not proven on a market scale. A first attempt is represented by the plant located in Zaragoza, which is able to provide affordable continuous operation, but, according to the TRL scale, the semi-industrial nature of the plant gives a TRL of 7 [27]. The Pyrum Innovations AG plant in Germany is already dimensioned to process a very big amount of feedstock, but is still operating at partial load since some parts of the reactor are still under testing procedures. Therefore, the waste tyre pyrolysis with moving bed reactor is classified with a TRL 8 [28]. From the economic point of view, waste tyre pyrolysis promises to be a very convenient process. Since the feedstock covers almost the 60% of the carbon black production processes, it is evident that using waste material abates this cost by a significant margin, with future projections of 0,8-1 $/kg [29].

1.3 Final considerations

Analysing all the described technologies for hydrogen and carbon black production, it is evident how all the conventional processes are cheap and convenient with respect to the green alternatives. However, they all rely on fossil fuels as feedstock, while the more innovative and greener solutions are all promising technologies for the decarbonization of the sector. What prevents them from establishing on the market are the higher production costs and the lower technology readiness level. In fact, most of the new technologies have proven to be feasible at laboratory scale but, as commonly happens in the innovation field, the new processes still have to be trusted by the bigger investors.

2. Carbon black and hydrogen co-production

Since both carbon black and hydrogen are valuable products with several industrial applications, it is interesting to investigate the methods that allow to produce them simultaneously. The chemical decomposition of methane through SMR has been used since a very long time to obtain hydrogen and, as seen in the previous chapter, is nowadays the most important pathway of hydrogen production. Unfortunately, SMR is also affected by the emission of 10 tons of CO_2 per ton of hydrogen produced. Water electrolysis is surely a good alternative for green hydrogen production, especially when low-carbon electricity is used. However, this process is extremely energy intensive, requiring at least 285 kJ per mole of H_2. For this motivation, the cost of the hydrogen produced via electrolysis is still quite high, preventing the large-scale commercial use of the technology [30].

On paper, the direct thermal decomposition of methane via pyrolysis could be a valuable environmentally friendly alternative. Even using conventional fossil generated electrical power the benefits in terms of CO_2 emissions would be huge, given the low amount of energy required for the reaction

$$CH_4 \rightarrow C + 2H_2 \quad 76\frac{kJ}{mol}.$$
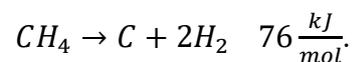
The big advantage of this production process is the possibility to obtain valuable CO_2 free solid carbon and hydrogen with much lower energy needs [31]. The most promising technologies in this field are the thermal plasma decomposition and the catalytic plasma decomposition, both of them exploiting the very high temperature reached by the plasma in order to break the methane molecule. In this chapter both the technologies will be presented, with deeper insights into the influence of the different reactor parameters on the final product characteristics.

2.1 Thermal plasma decomposition of methane

Research is being carried out in order to optimize the process, by making it less energy intensive and by improving the yield and the quality of the produced carbon black. The typical reactor configuration is shown in Figure 7
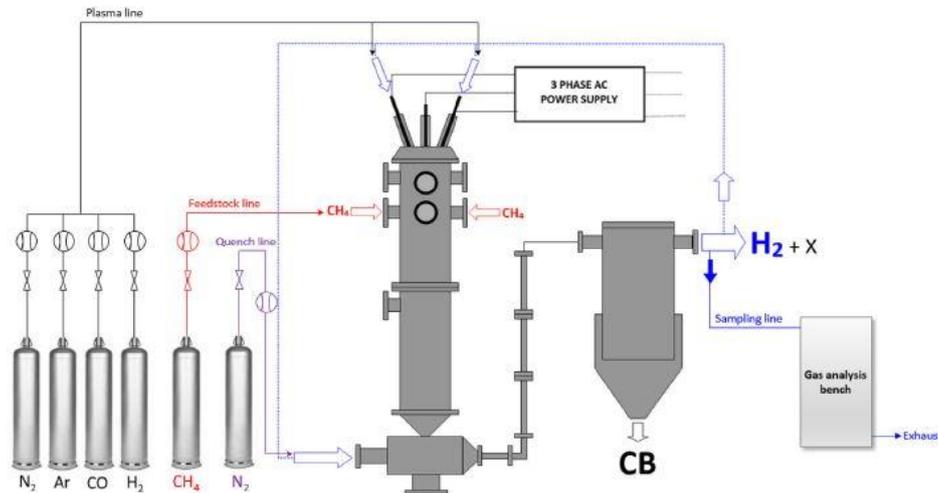
Figure 13 Reactor configuration for thermal plasma decomposition of methane [32]

The reactor is composed by the gas supply system, the plasma source, including the plasma line injecting the plasma gases into the reactor and the plasma torch, the pyrolysis reactor, the water cooling system, the filtering unit, usually a cyclone, and the gas analysis system. The plasma gas can be composed in many different ways, but firstly nitrogen or argon are introduced before methane injection to heat up the reactor until the thermal steady state is reached. Then, plasma gas composition and flow rate are progressively adjusted by adding hydrogen and/or carbon monoxide. Simultaneously, methane is injected into the reactor downstream of the plasma torch, starting the pyrolysis process. The plasma arc generated produces a plasma at typically 2000°C by the graphite electrodes, that are progressively consumed due to high temperature erosion. Due to erosion, the position of the graphite electrodes are continuously monitored and adjusted, even if the high thermal resistance of the graphite makes the process very slow. The final products are then separated into the filtering unit, where carbon black is captured and precipitated and hydrogen is free to reach the gas analysis system [30].

The kinetic model related to the system suggests two simple methods to increase the yield of products. The first one is to increase the pressure and so the molar concentration of reactants. The second one is to increase the nucleation rate by artificially introducing

nucleation sites with seeding techniques or, more simply, by adding more consumable graphite electrodes. The erosion that involves the electrodes would naturally introduce large amounts of solid carbon nucleation sites[32].
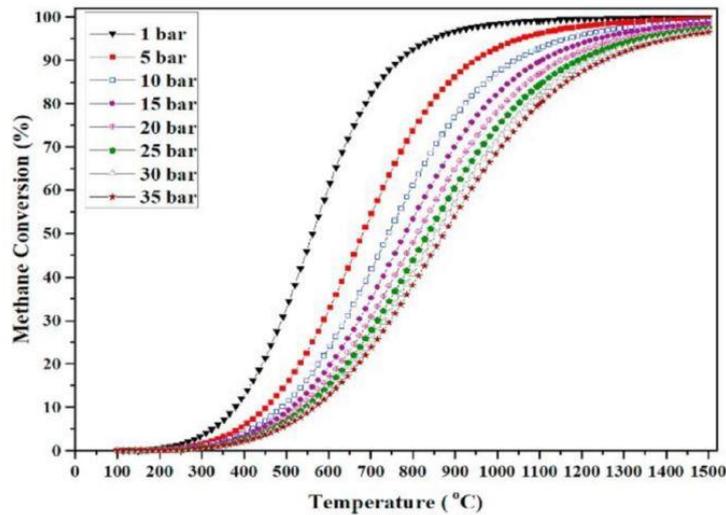
Figure 14 Methane conversion as function of reactor pressure[32]
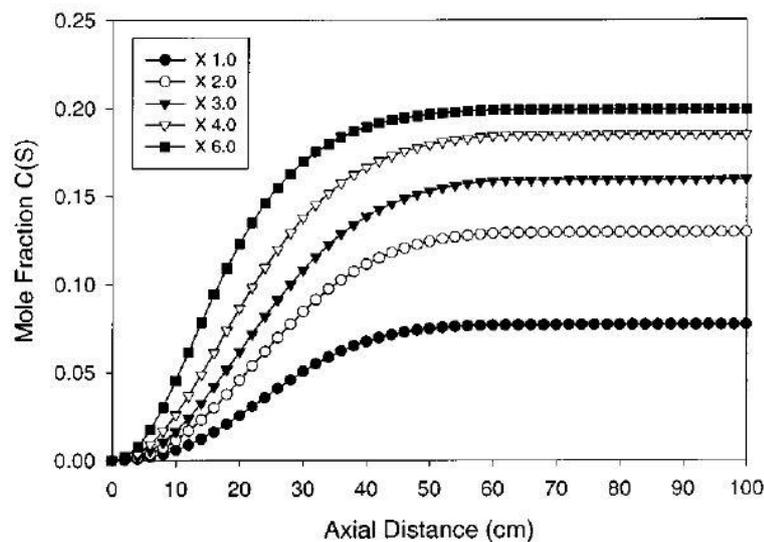
Figure 15 Carbon formation rates as function of nucleation sites[34]

With absence of catalysts, the thermal decomposition of methane produces mainly amorphous carbon black powders. The produced carbon is characterized by low crystallization levels, but more smooth and tidy structures can be formed at temperatures above 1500°C. Particle size increases with temperature as well.

2.2 Catalytic plasma decomposition

Even if the endothermicity of methane pyrolysis is moderate, temperatures of around 1200°C are required for thermal decomposition. Under different reactor configurations, a significant number of metal catalysts have been tested in order to lower the temperature of methane conversion. Nickel, iron and copper catalysts are all materials that show catalytic behaviour in the temperature range of 500-800°C [33]. These catalysts facilitate the production of carbon nanotubes and graphene [34]. The main limitations are the fast deactivation and the difficult separation from the products.

A valid alternative to face those problems is the use of carbon catalysts, whose activation temperature is in the range of 800-900°C. It takes much more time for a carbon catalyst to deactivate, but the catalytic activity is quite lower if compared to the one of metal catalysts[35].

The balance between formation, diffusion and precipitation on the catalyst is necessary to get stable growth, otherwise catalyst deactivation because of coking can occur. In particular, the excessive carbon deposited on the catalyst surface behaves as the coking agent that makes the catalyst performance degradate. Another cause of catalyst deactivation is the sintering phenomenon, in which the coalescence of catalyst particles enhances the loss of active surface and lowers catalyst performance.

2.2.1 Metal catalysts

Transition metals show good catalytic activity, which for non-supported catalysts is higher in nickel and cobalt rather than copper, iron, iridium and palladium. The field of solid metal catalyst is now focused on supported catalytic alloys, such as Ni-Fe/Al_2O_3. As mentioned previously, to optimize catalyst stability, the balancing between carbon formation, diffusion and precipitation is crucial to guarantee steady state nanocarbon growth. With this goal, Ni/Al_2O_3 catalyst can be doped with Fe in order to reduce the catalytic activity of Ni and make rates of carbon formation, distribution and precipitation balanced [34].

Another investigated alloy for catalytic methane pyrolysis is the Ni-Cu-Co. In the temperature range between 750 °C and 800°C the catalyst particles transitioned from spherical to semi-liquid and produced carbon nanotubes and shells, but immediately after

catalyst deactivation took place quite rapidly. Then, it was discovered that the semi-liquid catalyst particles formation can be limited by increasing the amount of Co into the catalyst composition [36].

Catalysts supports have also been investigated, in particular considering the loading of Ni onto TiO_2, Al_2CO_3 and $CaCO_3$ catalyst supports. By increasing the loading of Ni, methane conversion performance improved for TiO_2 catalyst, while the opposite happened to Al_2O_3 and $CaCO_3$ supports. This is because the TiO_2 support showed weak metal-support interaction, promoting the tip-growth mechanism that allows carbon extrusion from the active metal of the catalyst as the methane formation goes on. For the other two supports this phenomenon doesn't take place, leading to catalyst deactivation [33].

The carbon allotropes produced by a metal catalyst are of various nature and shape: graphitic carbon spheres, shells and carbon nanotubes [33]. As result of tip growth mechanisms, supported catalysts mainly produce carbon nanotubes [34]

2.2.2 Carbon catalysts

Carbon catalysts show quite low catalytic effect, that mainly depends on the porosity of the catalyst itself. The amount of deposited carbon is generally at least one order of magnitude smaller than metal based catalysts [35].

The growth potential of the filamentous carbon is typically related to the presence of metal impurities into the carbon catalyst. Pure carbon black catalyst enhances the formation of ordered crystalline structures, with no formation of filamentous or fibrous structures. Combined activated carbon and carbon black catalyst increases the crystallinity and graphitization of the produced carbon, but also filamentous and fibrous structures are observed [37].

2.3 TRL and production cost

Thermal plasma decomposition have been used for very long time in the past to produce the thermal black. In the 90s Norwegian company Kvaerner (now Akker-Kvaerner) worked to the development of a DC plasma plant for the co-production of hydrogen and carbon black from natural gas. The first industrial unit was built in Canada in 1997, with a capacity of

20,000 tonnes of carbon black and 6,000 tonnes of hydrogen per year. Further development of the technology was abandoned in 2003 due to technological issues and the poor quality of the carbon black produced. In 2012, the Californian startup Monolith Materials Inc. began a collaboration with PERSEE team at MINES ParisTech to develop a first 1 MW pilot plant, tested from 2013 to 2018. Then, in 2018 the company started the construction of the first industrial production plant in Nebraska, with a capacity of 14,000 tons of carbon black and 4600 tons of H_2 per year [38]. In April 2024, Monolith and Mines Paris-PSL extended their research partnership until February 2030 to advance thermal plasma processes for low-emission carbon black and hydrogen production [20], [29].

So, even if the carbon black quality and the technological issues are still a concern, more and more research has been conducted and is being carried out by synergies of private companies and institutions, making the technology slowly spreading in the hydrogen and carbon black markets. According to the TRL criteria, the readiness level of the technology is equal to 9. The production cost of the hydrogen is in the range from 1,7 to 4,5 $/kg, while the carbon black cost goes from 0,8 to 1,1 $/kg [39].

2.4 Final considerations

Methane decomposition is a viable and well-known technology for the hydrogen and carbon black co-production. The technological problems and the poor carbon black quality related to the first attempts of industrial scale-up have represented a difficult obstacle in the past. However, there seems to be a big interest for the technology by the bigger investors, making it possible to create synergies between academic and research institutions with private companies. This cooperation looks very promising to fix the issues and to finally allow the establishment of the technology in the market.

The co-production of carbon and hydrogen from methane is once again a process that relies on a fossil fuel as feedstock. A very interesting alternative that could solve this problem is the use of plastic waste, an inexpensive material whose end of life use or disposal is commonly considered as a problem rather than a resource. Plastic waste gasification is the most promising technology to obtain both the products on which the work is focused, but right now is still developed only at laboratory scale.

3. Plastic waste gasification

Plastic waste gasification is a well known technology in the field of the green fuels production. In the last years, it is also being evaluated as an alternative method for the co-production of carbon black and hydrogen, creating the possibility of using a waste material to produce valuable products without the dependence on the methane price. In this chapter the most promising production processes individuated at laboratory scale are presented, along with the main operating parameters that influence the production rate and the product quality.

3.1 Two-stage catalytic gasification of plastic waste

Pyrolysis and gasification have proven to be two valid techniques for the conversion of plastic waste into fuels and chemicals. Gasification allows to obtain hydrogen and syngas with the possibility to employ plastic materials of different compositions, but high tar formation is still a challenge to be faced. Pyrolysis has the advantage of simultaneously producing hydrogen rich syngas and carbon nanotubes. However, the different chemical composition of the plastic feedstock represents the main obstacle for this technology [40]. The use of catalyst and the adoption of a two-stage catalytic pyrolysis process make the system more efficient, allowing to obtain higher hydrogen yield [41].
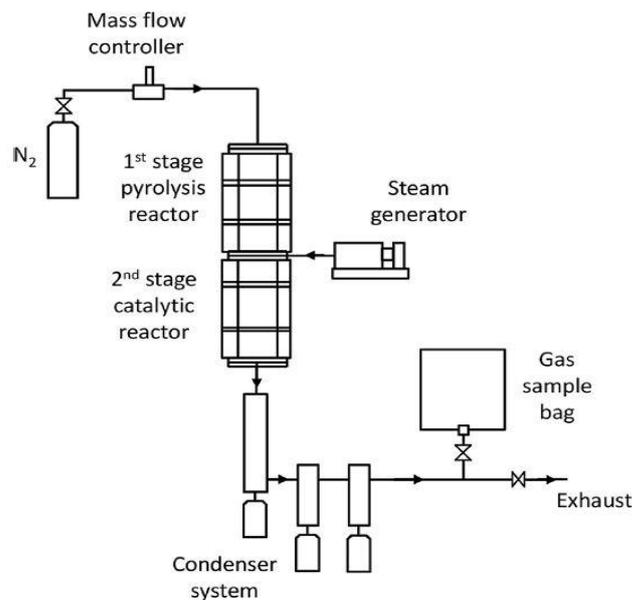
Figure 16 Fixed bed system for plastic catalytic pyrolysis [44]

The working principle of the system is to thermally crack the plastic feedstock in absence of oxygen, typically at a temperature of 500-700°C. The obtained pyrolysis gases are passed to the catalytic stage, that operates at higher temperature (800-900°C) to produce hydrogen-rich syngas, while different carbon allotropes are deposited on the catalyst. The gases obtained at the end of the catalytic process are cooled down in a condenser system that allows to remove condensable hydrocarbons [42]. The process conversion efficiency can be affected by many variables and parameters, including the possibility of steam injection in the catalytic stage, whose improvement and optimization are still being studied at laboratory level.

3.1.1 Effect of catalyst

Catalysts are able to promote the formation of gaseous products and decrease the oil yield. Ni and Fe catalysts are the most commonly used because of their good activity for hydrocarbon conversion and low cost. As for catalysts used in methane pyrolysis, coke deposition and sintering are the main causes of deactivation, but they can be avoided by enhancing coke gasification using a fluidized bed reactor [43]. Similarly to what has been detected in the catalytic pyrolysis of methane, Ni-Fe/Al_2O_3 bimetallic catalyst allows to obtain the highest hydrogen yield (42 mmol H_2/g plastic) thanks to the strong interaction between catalyst and support. Among all the Ni-Fe molar ratios investigated, the best results have been achieved with the Ni-Fe 1:3 [44]. Further improvement in hydrogen yield (66 mmol H_2/g plastic) have been reached with the use of zeolite-supported Ni catalyst, thanks to the lower susceptibility of zeolite to coke formation [45].

Carbon nanotubes (CNTs) produced by hydrocarbon pyrolysis can have different morphological characteristics depending on the metal catalyst and the metal support used. Using real world plastic waste, CNT diameter was discovered to be governed by catalyst particle size: the smaller metal particle size in Ni/γ-Al_2O_3 produced a smaller outer diameter (20 nm) than the one of the deposits formed on Ni/α-Al_2O_3 (40-50 nm) By substituting Fe to Ni, given the better solubility of carbon in Fe, higher amount of carbon was obtained. Furthermore, Ni/γ-Al_2O_3 catalyst gave as a product the largest amount of filamentous carbon (287 mg/g plastic) and a smaller quantity of amorphous carbon (120 mg/g plastic). The yield and quality of CNT increased with the porosity of the alumina support, so α-Al_2O_3 generated more carbon deposits [46].

3.1.2 Effect of temperature

Temperature has a very important influence on the pyrolysis products: at low temperature hydrocarbon conversion is incomplete and lower gas production is performed. At higher temperatures, hydrogen yield is increased at expenses of methane and other gaseous hydrocarbons [47]. With the Ni-Fe/γ-Al2O3 catalyst, by increasing the temperature from 700°C to 900°C, the hydrogen yield increased from 27 mmolH$_2$/g plastic to 43.7 mmolH$_2$/g plastic. Similarly, employing the Ni/Zeolite catalyst, hydrogen yield increased from 43.02 mmolH$_2$/g plastic to 66.09 mmolH$_2$/g plastic by increasing the temperature from 650°C to 850°C [46]. At temperatures below 700°C the dominant reactions are related to hydrocarbon decomposition, while at higher temperatures water gas shift reactions between H$_2$O and CO are enhanced, decreasing hydrocarbon concentration and coke deposition rate. Furthermore, at high temperatures gasification of the deposited coke is enhanced as well [48].

An increase of catalysis temperature causes also the increase in the production of filamentous carbon with larger diameters, due to the agglomeration of the metal particles of the catalyst. At the same time the higher temperature increases the supply of pyrolysis gases, causing excessive carbon feeding and, consequently, catalyst poisoning [41]. At lower temperatures (700°C) straight filamentous CNTs are produced, while multi-walled CNTs with a more heterogeneous variety of diameters and shape are obtained at 800°C. High pyrolysis temperature enhances free radicals formation and dissociation of hydrocarbons, leading to an increase in CNT yield. The maximum yield has been obtained at a temperature of 700°C [49].

3.1.3 Effect of steam injection

Steam injection during plastic pyrolysis enhances hydrocarbon reforming and influences the final gas composition. With Ni-Fe/γ-Al2O3 at 800°C, by going from the absence of steam injection to a steam injection with steam/plastic ratio of 2.6, the hydrogen yield increased from 31.8 mmolH$_2$/g plastic to 92.7 mmolH$_2$/g plastic. An increase in the overall gas yield was also observed due to the enhancement of steam reforming reactions, while the hydrogen concentration remained stable between 62% to 65% of the total gas composition. The increase of the reforming reactions leads to a decrease of the heavier hydrocarbons and the increased gasification of deposited coke slows down the catalyst deactivation [46].
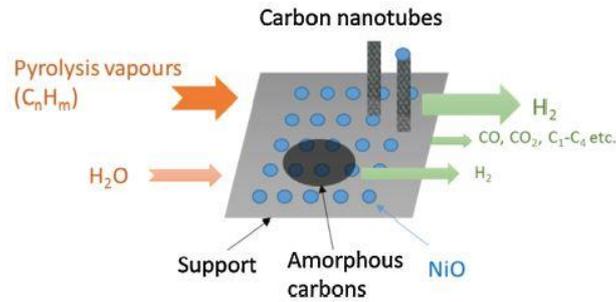
Figure 17 Working principle of the catalytic stage with steam injection[34], [42]

Injection of steam has proven to be very beneficial for hydrogen production. However, the same thing can not be said for CNTs production, since when steam is added in the reactor both amount and quality of carbon deposits decreased, being mainly filamentous. Referring to the steam/plastic ratios previously mentioned, CNTs production decreased from 287 mg/g plastic to 17 mg/g plastic for 0, 0.3 and 1 ratios. With a steam/plastic ratio of 2.6 almost no CNT was produced, since all the deposited carbon reacted with steam [46].

3.1.4 Effect of feedstock

The main feedstock parameter affecting the hydrogen production are the purity of the material and the different compositions of the plastic wastes. Polystyrene (PS), polyethylene (PE) and polypropylene (PP) are all suitable materials for pyrolysis, while PVC and PE are still difficult to be introduced into the process. Polyolefins, like PP, allow to obtain maximum hydrogen production, while PS and PE give a much lower amount. This is because in the original composition of these two plastic materials the quantity of hydrogen is smaller [50].

In PS pyrolysis the deactivation rate of the catalyst is observed to be quite faster if compared to the other plastic feedstocks. The best catalyst in terms of minimization of the differences between reaction rates with different feedstocks is, up to the current research advancement, the ruthenium (Ru) catalyst, characterized by high activity. By feeding PS and PP at the same temperature gas yield has been observed to be almost the same for both of them, despite the different composition [51].

With a wide range of different feedstocks tested, the main solid product is filamentous carbon. During continuous pyrolysis and in-line steam reforming over Ni catalyst, encapsulated type coke can obtained for PS, while with the same reactor setup filamentous

carbons are produced with PE. In more recent studies, the type of feedstock has proven to influence the carbon shape: filamentous carbon is observed for polyolefins, while encapsulating coke is produced with PET and PS [50]. Also the reaction atmosphere can change the carbon production, since CO_2 injection to the feedstock leads to the reaction with the carbon deposits, forming CO. At low temperatures, below 500°C, the effect of feedstock on CNTs yield and production results to be even more relevant [41].

3.2 Thermal cracking of plastic pyrolysis syngas

Another method that allows to contemporarily obtain hydrogen and carbon black is the plastic waste pyrolysis followed by the thermal cracking of the obtained syngas. This process allows to obtain the products without using any catalyst, avoiding the problems related to cost and performance degradation typical of catalytic processes [52].
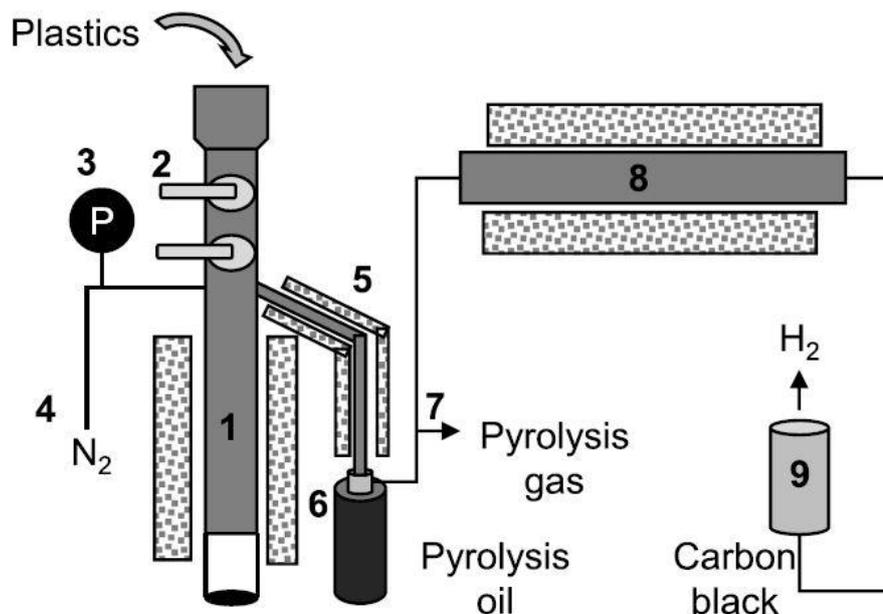
Figure 18 Experimental setup for thermal platstic pyrolysis

In this process both nitrogen, used as sweep gas, and plastic waste flakes are fed into the pyrolysis reactor (1) pre-heated at 600°C. Differently from what seen in the gasification process explained before, in this case the resulting volatile products are sent to the condenser by hollow tube at the same temperature, in order to increase the residence time and facilitate their thermal decomposition into pyrolysis gas. The pyrolysis gas is composed by carbon monoxide, carbon dioxide, nitrogen, methane and other C_2-C_5 alkanes. The liquid pyrolysis

44

oil is collected into a condenser kept at ambient temperature (23°C), while the pyrolysis gas is sent into the thermal reactor where it is heated up to 1300°C. The very high temperature allows to obtain the thermal decomposition of the hydrocarbons contained in the gas into carbon black and hydrogen without using any catalyst. Finally, the carbon black is separated from the final obtained syngas with a bag filter [52].

3.2.1 Effect of temperature and feedstock

Pure LDPE (Low Density Polyethylene) was used as a reference material in the reference study [52]. The main output was oil (52 wt%) followed by solid carbon (40 wt%), product gas (9 wt%) and negligible quantity of solid residue remaining in the pyrolysis reactor (<0.1 wt%). Commercial pyrolysis processes optimized for oil production can produce 75–95 wt% oil, but, in this particular case, oil production was lower due to higher pyrolysis temperature and increased residence time, that enhanced the formation of pyrolysis gases. Hydrogen production from LDPE was 7 wt%. Pure LDPE and a mixture of other plastic packaging, mainly composed of polyethylene and propylene, were also used to perform different experiments and assess all the effects related to temperature and feedstocks. Polyethylene Terephthalate (PET) bottles were added to the mixed plastic to investigate PET influence on hydrogen and solid carbon production. LDPE was used in the form of pellets, while the mixed plastics and the PET were shredded into flakes before the experiment start.

With respect to LDPE, the mixed plastic with and without the added PET resulted in the formation of more solid residue and less oil, while the oil composition is comparable regardless the feedstock. This lower oil yield has already been documented in literature and is mainly correlated with increased formation of CO and CO_2 from PET [53]. Another reason is the production of sublimated organic solids, like benzoic and terephthalic acids, that condense on cold reactor walls or form aerosols, which by-pass the oil trap and accumulate in downstream gas lines. This peculiarity is particularly evident for what concerns the mixed plastics with addition of PET, the product gas yield is by far the highest among all the other feedstocks (21 wt%), but the hydrogen yield is the lowest (5 wt%). Pure LDPE showed better mass balance closure (101%) as compared to other two samples (80–99%, depending on the experimental run). The decrease in mass recovery suggests that in case of real waste samples there could be other unaccounted compounds formed during the process, for example the

volatile organic compounds or aerosols condensing along the lines. The purity of H_2 gas is negatively influenced by polyethylene terephthalate in the feedstock due to the dilution of gas by CO. For both LDPE and mixed plastics, the total amount of hydrocarbon compounds obtained from pyrolysis is 41-84 vol%, while the hydrogen concentration ranges only between 7 and 12 vol%, depending on the different feedstocks and temperatures. The higher ash content in in the experiment with mixed plastics could be related to the presence of inorganic fillers and metallized packaging in the plastic waste. The decomposition of methane contained in the pyrolysis gas is the limiting reaction step during H_2 production and it is improved at higher thermolysis temperature.

Although the volumetric percentages of the above mentioned impurities are lower compared to hydrogen, these compounds are heavier. Therefore, even small volumetric concentrations of impurities can make a large impact on the yield of product gas expressed on a mass basis. The contribution becomes increasingly evident with the increase in concentration of gas impurities as it can be observed in case of the product gas. The volumetric hydrogen concentration in the product gas was the highest in case of LDPE ($94,2 \pm 0,7$ vol%) followed by mixed plastics ($91,3 \pm 1,7$ vol%) and mixed plastics added with PET ($74,3 \pm 2,9$ vol%). CO_2 was present in the pyrolysis gas of all samples and, after thermolysis at 1300 °C, it was converted into CO, indicating the oxidation of hydrocarbon compounds and solid carbon by CO_2 in the thermolysis reactor. For all samples, almost complete decomposition of C_1-C_5 hydrocarbon compounds is achieved at 1300°C. Methane is proven the most stable at high temperatures, given the highest volumetric concentration. In fact, compared to hydrocarbon compounds with larger number of carbon atoms, methane has the stronger C-H bond, making it more difficult to decompose into C and H_2 [54]. The output of pyrolysis gas was 600–800 mL/min, depending on plastic feedstock. Given all the previously cited phenomena taking place in the thermolysis stage, the decomposition of hydrocarbon compounds into solid carbon and hydrogen takes place with each CO_2 molecule producing 2 molecules of CO during the reaction with hydrocarbon compounds and solid carbon. Due to these reactions, the volume of product gas after thermolysis increased to 1000–1350 mL/min, depending on the feedstock. In all gas samples, hydrogen is the main component with the lowest concentration at 1200°C ($89,8 \pm 0,4$ vol%), and the maximum at 1400°C ($94,0 \pm 0,5$ vol%). The contents of N_2 and CO were 3,0–4,9 and 1,8–3,0 vol%, respectively at 1200–1500°C. Among hydrocarbon compounds, methane is the predominant species due to the high

stability of the molecule. The largest methane content is observed in the product gas obtained at 1200 ∘C (4,1 ± 0,5 vol%) followed by 1300 ∘C (1,0 ± 0,3 vol%), 1400 ∘C (0,1 ± 0,1 vol%) and 1500 ∘C (0,1 ± 0,1 vol%). The concentration of C_2-C_5 hydrocarbon compounds at 1200 ∘C was 0,3 vol% and doesn't exceed 0,1 vol% at higher temperatures. According to these results, at the studied temperatures, the decomposition of methane was the limiting step determining the overall conversion efficiency of hydrocarbon compounds in plastic pyrolysis gas into hydrogen. For the experimental setup and conditions used in the study, almost complete hydrocarbon conversion contained in the pyrolysis gas was achieved at around 1400°C.

3.2.2 Characterization of the solid carbon

Solid carbon is the main by-product from hydrogen generation and is the most abundant output from the thermolysis of plastic pyrolysis gas regardless of the plastic type and process temperature. Characterization of solid carbon is important for determining potential applications of this material to improve economic viability of the plastic waste-to-hydrogen process. The morphologies resulting from the thermal decomposition of hydrocarbons is different from the ones synthesized via catalytic chemical vapor deposition of pyrolysis gas from plastics at lower temperatures. As seen in the previous chapters, the typical carbon products of catalytic processes consist in filamentous carbon, such as multi-walled carbon nanotubes, few-walled carbon nanotubes and nanofibers. Solid carbon collected from the particle filter of the experiment consisted of spheroidal aggregates, resembling typical morphology of carbon black. Taken into consideration the residence time of product gas in the thermolysis reactor (9–14 s), the formation of carbon black aggregates is accomplished within several seconds. Solid carbon recovered from the thermolysis reactor was predominantly composed of fused spheroidal particles coated with a layer of attached pyrolytic carbon.

3.3 Final choice of the process

The two stage catalytic gasification and the thermal pyrolysis are the processes that allow the co-production of hydrogen and carbon nanomaterials.

The first one allows to obtain hydrogen with a purity that doesn't exceed 65% and carbon nanotubes. The obtained carbon nanomaterials are captured and fixed onto the porous structure of the catalyst along with liquid residues and there are no reported methods to obtain the separated products. The main strong point is the reduced operating temperature (700-900°C), corresponding to a lower energy consumption. On the other hand, the high cost of the catalyst, the fast catalyst deactivation and the difficulties in its regeneration make the process to be still not ready for a continuous production regime and, for now, for a future scale up. Plastic pyrolysis followed by the thermal cracking of the pyrolysis gas doesn't require any catalyst to be carried out, preventing the system from all the related problems. Moreover, in the case of LDPE and mixture of LDPE and PP, the hydrogen purity is very high and the carbon nanomaterials resulting from the thermal cracking stage is proper carbon black. The only disadvantage of the absence of catalyst consists in the necessity of higher temperatures (1200-1400°C), increasing the operating costs of energy consumption.

Considering all these factors, the pyrolysis of plastic followed by the thermal cracking of the pyrolysis syngas has been chosen to model the possible upscale of the process at industrial level.

4. Model development

The model of the system has been implemented on the Aspen Plus software, which is suitable for modelling steady state processes. The goal of the Aspen Plus model is to quantify the quantity of products obtained and the energy demand of the entire system. Further thermal integration with Aspen Energy Analyzer has been performed in order to explore the possibilities of a decrease in the input thermal demand, which is quite high considering the temperatures reached in the thermolysis stage. Finally, to assess the feasibility of the industrial scale-up of the process, a techno-economic analysis is carried out to find the Levelized Cost Of Hydrogen (LCOH) given by the plant and to compare it to the LCOH of the current technologies adopted on large scale for hydrogen production.

4.1 Methods and assumptions for the Aspen Plus simulation

Plastic waste has been defined on Aspen Plus as a non-conventional material, so the enthalpy and density of the several flows of the process have been calculated using HCOALGEN and DCOALIGT models, that require as input the proximate and ultimate analysis of the inlet feedstock. The plastic waste pyrolysis has been modelled in two steps: the first one is a fictitious yield reactor ('DECO') required to decompose the unconventional plastic waste inlet into its different atoms, according to the ultimate analysis. Because of the absence in literature of kinetic parameters related to plastic waste pyrolysis, the stoichiometric reactor ('PYRO') has been inserted in order to obtain the desired amount of C_1-C_5 hydrocarbons in the pyrolysis gas and replicate the results of the laboratory experiment of the paper [52] . The process is assumed to be carried out at steady state, without pressure losses along the lines and in the reactors. In the reference paper is also reported that, given the dimensions of the reactor and product gas volume provided in the reference paper, it can be concluded that the thermolysis time was sufficient to decompose most of methane containing in the pyrolysis gas. As a consequence, the thermolysis reactor has been modelled with a Gibbs reactor, whose output is the product obtained at equilibrium.

For the energy fluxes calculations, if a single real reactor is split in two distinct reactors in the simulation for software modelling reasons, the total thermal demand of the single real reactor is determined as the sum between two separate thermal demands resulting from the

simulation. The operating pressure of the entire system is 1 bar, without any pressure loss along the process.

Firstly, the inlet feedstock must be defined. The material used for the simulation is LDPE, as for the reference article. The proximate and ultimate analysis are the necessary input data for Aspen Plus to model plastic waste into the simulation as unconventional material and determine its properties.

Element	Wt%
C	83,82
H	15,2
N	0,09
O	0,8
Fixed carbon	0,1
Volatile matter	99,8
Ash	0,09

Table 5 Ultimate analysis of LDPE

Element	Wt%
Fixed carbon	0,1
Volatile matter	99,8
Ash	0,09

Table 6 Proximate analysis of LDPE

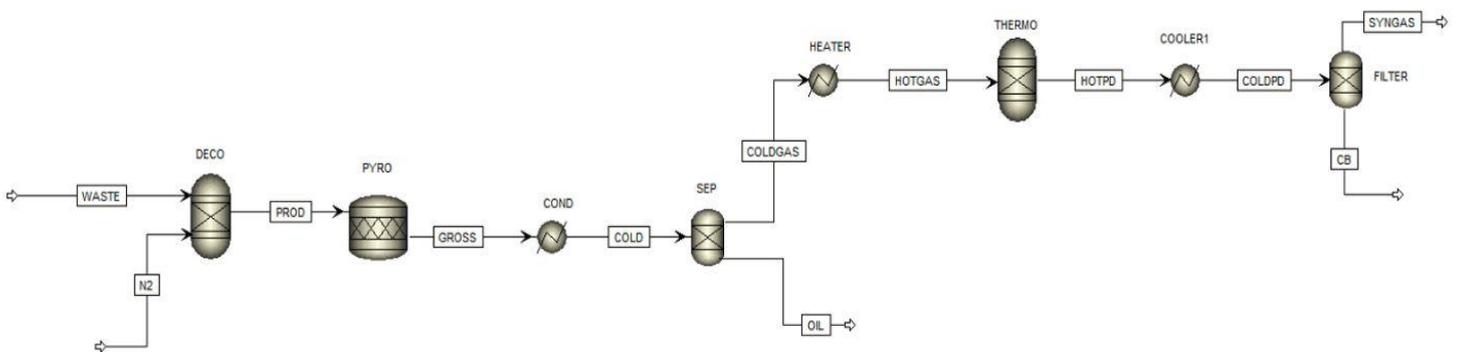The model developed on Aspen Plus is shown in Figure 19:

Figure 19 Aspen Plus model

As previously explained, the pyrolysis reactor is modelled with the two 'DECO' and 'PYRO' reactors, that allow Aspen Plus to respectively decompose the plastic waste into its elemental components and to obtain the desired yield of pyrolysis products. The nitrogen and plastic waste inlet flows are at a temperature of 25°C, while the two reactors work at 600°C. The energy demand of the 'DECO' reactor is positive, so it means that the thermal decomposition of plastic waste is an endothermic phenomenon. On the other hand, the thermal demand of the 'PYRO' reactor is negative, so it means that the reactions that lead to obtain the pyrolysis products are exothermic.

The operating temperature required for the condensation of the heavier hydrocarbons contained in the pyrolysis products is 23°C, so the flux must be cooled down. The condensation process is modelled with a separator, in order to control the product yield and maintain the compliance with the experimental results of the paper.

The thermolysis stage requires very high temperatures (1300°C) and a pre-heating of the gas would help to decrease the thermal demand of the thermolysis reactor. To thermally optimize the system and decrease this demand, a pre-heater is installed immediately after the cold trap to increase the temperature of the pyrolysis gas up to 550°C before entering the reactor. The temperature of pre-heating has been selected low enough to prevent the bigger and less stable hydrocarbons to crack before entering the proper reactor. The implementation of further thermal optimization of pre-heating through Aspen Energy Analyzer is explained in the next section. The thermolysis results in the production of hydrogen and carbon black from the different hydrocarbons present in the pyrolysis gas.

The separation of carbon black is carried out by means of polyester bag filters, able to withstand temperatures up to 150°C and a very various range of chemical and humidity conditions [55]. Since the products exit the thermolysis reactor at 1300°C, a cooler is inserted before the filters to decrease the products temperature down to 130°C and guarantee the correct operating temperature.

A comprehensive resume of all the relevant properties of the fluxes involved in the process is reported in Table 7:

Flow name	Mass flow (kg/s)	Composition (wt%)	Temperature (°C)	LHV (MJ/kg)
WASTE	0,405	See Table 5	25°C	44
PROD	0,421	C 80,6% N_2 3,9% O_2 0,8% H_2 14,6%	600°C	42,3
GROSS	0,421	C 58,7% N_2 3,9% H_2 8,3% CH_4 17,5% C_2-C_5 10,3%	600°C	42,8
COLD	0,421	Equal to GROSS	23°C	42,8
COLDGAS	0,205	C 33,9% N_2 7,9% CH_4 35% C_2-C_5 20,7% CO 1,3% CO_2 1,1%	23°C	38,3
OIL	0,216	C 82,8% N_2 0,8% H_2 16,4%	23°C	46,7
HOTGAS	0,205	Equal to PRODGAS	550°C	38,3
HOTPD	0,21	C 76,6% N_2 7,9% H_2 12,5% CH_4 0,12% CO 2,7%	1300°C	34,2
COLDPD	0,205	Equal to HOTPD	130°C	34,2
CB	0,16	C 100%	130°C	32,7
SYNGAS	0,045	N_2 33,8% H_2 54% CH_4 0,53% CO 11,6%	130°C	66,2

Table 7 Main properties of the process fluxes

4.1.1 Insertion of pressure swing adsorption reactor

All the present literature about the plastic pyrolysis for hydrogen production has as a final result a hydrogen-rich syngas and not pure hydrogen for fuel cells, that can be assessed as the most important end use of hydrogen in energy applications. The 94,2% hydrogen purity is a very high value if compared to the hydrogen purity obtained with catalytic processes, but still much lower than the one required for fuel cells (> 99,99%). Pressure swing

adsorption (PSA) is a technique that allows to obtain gases at very high purity at a relatively low cost. The PSA is a process carried out in different steps characterized by different pressure levels: adsorption, desorption and pressure equalization. The adsorption takes place at high pressure and allows the small H_2 molecules to pass the molecular sieve, while the bigger molecules remain trapped. Once the molecular sieve reaches saturation, pressure is reduced, allowing the adsorbed molecules to detach and to effectively cleaning the sieve for the next cycle. To reduce gas wastage, a portion of syngas from the pressurized tower is transferred to the other tower until the pressures are equalized, but, when very high purity is required, also a portion of the product gas is transferred. By alternating between these stages in two towers, PSA systems maintain a continuous flow of the desired gas with a reduced energy input. The choice of molecular sieve, cycle timing, and system pressure all contribute to the effectiveness in producing high-purity gases [56]. The hydrogen recovery, expressed as the ratio between the mass of hydrogen in the inlet syngas and the mass of pure hydrogen leaving the PSA unit, is considered to be 0,9 [57].

4.2   Methods and assumptions for the economic analysis

The final aim of the project is to evaluate the economic feasibility of a possible scale-up of the plant, in order to understand the potential of the technology at industrial level. To do that, all the capital and operational expenditures for the purchase of the equipment and for the energy and maintenance costs during the useful life of the plant have been estimated. The final result of the analysis is the LCOH (Levelized Cost of Hydrogen), so the cost of hydrogen that allows to obtain a NPV (Net Present Value) equal to zero at the end of the plant life. Once the LCOH is found for the reference conditions, a sensitivity analysis changing the parameters of energy cost, interest rate, debit fraction on the initial investment and carbon black commercial value is finally performed to assess the influence of each one on the final LCOH.

4.2.1 CAPEX calculation

The capital cost has been evaluated through the method proposed by the NETL (National Energy Technology Laboratory) [58]. Bare Erected Cost (BEC) includes the cost of process equipment, on-site facilities, infrastructure supporting the plant, and the direct/indirect

labour required for construction and installation. Indirect expenses comprise all equipment and material transportation costs, construction overhead, and engineering expenses. The second cost level is engineering, procurement, and construction cost (EPCC), which consists in the cost of contractor services, including detailed design, contractor permitting, and project management costs. These services are estimated at 20 % of BEC. Total plant cost (TPC) accounts for BEC, EPCC, process and project contingencies (unpredicted costs related to the complete project definition and engineering). Contingency costs include time delays and unpredicted price increases. The aim of contingencies accounting is to cover project uncertainties, as well as the cost of any additional equipment required during the plant manufacturing. Process contingencies are considered to be 5% of BEC, while project contingencies are calculated as the 20% of the sum between EPCC and process contingencies.

The total overnight cost (TOC) include all the other necessary expenses resumed in Table 8:

Expense	Value
PPC Pre production cost	2% of TPC
INC Inventory capital	0,5% of TPC
LND Land cost	6889 €/hectare
FNC Financing cost	2,7% of TPC
OOC Other owner cost	15% of TPC
TOC Total overnight cost	TPC+PPC+INC+LND+FNC+OOC

Table 8 Methodology for the TOC calculation

The most important expense reported in the table is the OOC (15 % of TPC), that accounts for preliminary feasibility studies, local economic development, infrastructures outside of site boundaries, legal fees, and owner's engineering. The equity share of TOC represents the first negative cash flow at the beginning of the financial analysis [58]. For each component, the BEC is evaluated on the basis of the prices of commercial samples or calculated with the empirical correlations provided by Turton et al.[59]. The empirical correlations adopted are valid for the year 2001, so a correction based on the CEPCI (Cost of Energy Plant Index) [60] has been performed to take into account the increase of the cost of the same components over the years:

$$\frac{Cost_{2025}}{Cost_{2001}} = \frac{CEPCI_{2025}}{CEPCI_{2001}}$$

The generic correlation suggested in literature to find the cost of the component C_p^0 is the following:

$$\log_{10} C_p^0 = K_1 + K_2 \log_{10}(A) + [K_3 \log_{10}(A)]^2$$

With K_1, K_2, K_3 defined as constant numbers changing from component to component and A standing for the reference sizing parameter.

According to the NETL methodology previously explained, knowing the total BEC of the plant components it is now possible to calculate the TOC, so the total CAPEX of the plant.

$$TOC = EPCC + PJ + PC + PPC + INC + LND + FNC + OOC$$

4.2.2 OPEX calculation

The operational costs are identified as the costs necessary to run the plant and to guarantee its correct maintenance. The elements of the plant requiring energy are the pyrolysis reactor, the thermal reactor and the PSA unit, with the energy consumptions of the first two known from the Aspen Plus simulation and with the assumption of 80% efficiency for the pyrolysis reactor and 85% efficiency for the heating elements of the thermal reactor. The PSA unit consumption of $1,2 \frac{kWh}{kg \, H_2}$ has been estimated from literature parameters, depending on the hydrogen purity at the inlet of the process, the flow rate and the range of pressure swing [64].

The pyrolysis reactor requires heat in order to carry out the pyrolysis process and is fed with natural gas. For the gas cost, the average European value of October 2025 is taken as a reference and is equal to 32 €/MWh [65]. For the electricity cost, the average value of October 2025 in the Italian market is taken as a reference and s equal to 116 €/MWh [66]. The cost of the water needed to satisfy the cooling demand is 0,65 €/m^3 [67].

In the OPEX accounting, at the tenth year are also added the expenses related to the substitution of the pyrolysis reactor and the bag filters.

4.2.3 Calculation of the final LCOH

Other than capital and operational costs, also the annuity and taxes payments have to be taken into account for the final LCOH calculation. The annuity An related to the repayment of the initial debt is calculated as:

$$An_k = TOC * Xd * \frac{r * (1 + r)^k}{(1 + r)^k - 1}$$

The negative cash flow related to taxes Tx, calculated with a tax rate r_{tax} of 26% [71] with the following expression, that takes also into account the interest expenditure IE_k and the depreciation cost DEP_k of the components (considered to be the 1% of the BEC of each component [58]):

$$Tx = r_{tax} * (Rev_k - Exp_k - IE_k - DEP_k)$$

Finally, the LCOH is calculated as :

$$LCOH = \frac{CAPEX + \sum \dfrac{Total\ annual\ costs}{(1 + r)^k}}{\sum \dfrac{H_2}{(1 + r)^k}}$$

The NPV at the year k is calculated as:

$$NPV_k = -C_0 + \sum \frac{CF_k}{(1 + r)^k}$$

Where the total cash flow $CF = Rev - Exp - An - Tx$ takes also into account the total revenues coming from the hydrogen and carbon black selling.

5. Results

In this section are shown all the results obtained for both the Aspen Plus simulation and the economic analysis. The possibility of thermal optimization and integration for the cooling demand have been assessed with a model developed on Aspen Energy Analyzer, with beneficial effects on the overall process efficiency. The economic analysis is focused on the final LCOH obtained for the process carried out in reference conditions. Then, the sensitivity analysis is performed, varying the parameters of carbon black selling price, electricity cost, interest rate and debt fraction on the initial investment to evaluate their impact on the LCOH.

5.1 Aspen Plus model results

The Aspen Plus model results were analysed for what concerns the energy demands of the several components of the plant and the final syngas yield and composition, with particular attention to hydrogen purity. The process identified for the scale-up is purely thermal, without the adoption of any catalyst or steam injection, making necessary for the thermal cracking of hydrocarbons into carbon black and hydrogen very high temperatures and the total energy demand for the process to be quite big. The efficiency of the burner necessary for the pyrolysis to take place in the reactor is fixed to 80%, as well as the one of the electric heater present into the thermal reactor. For what concerns the plastic waste pyrolysis, the energy required to pyrolyze 1 kg of material is approximately 840Wh [68]. The result obtained on Aspen Plus is very close to this value (837Wh). All the other energy fluxes referred to 1 kg of plastic waste inlet feedstock, both at heating and cooling sides, are resumed in Figure 20:
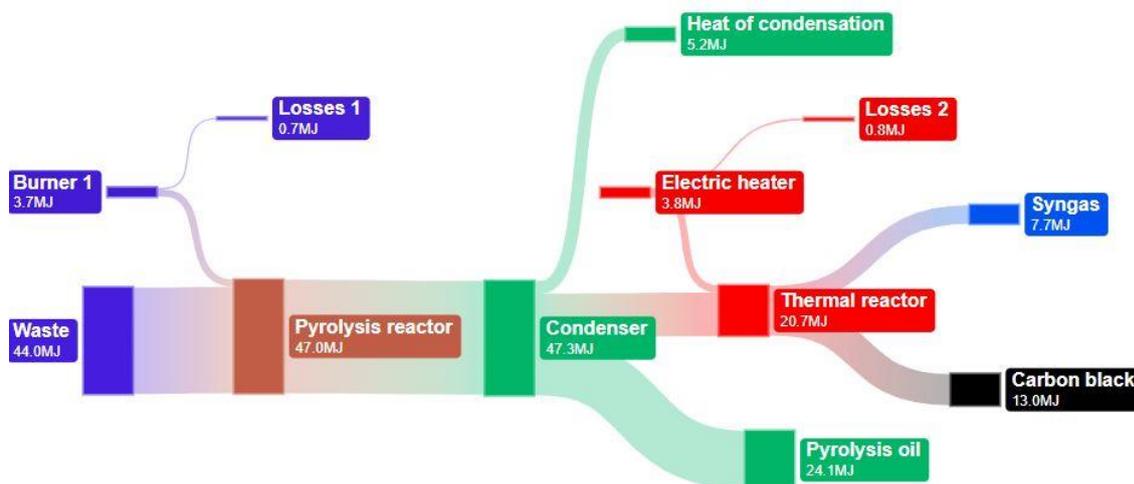

Figure 20 Sankey diagram of energy fluxes

The LHV of the plastic waste calculated in the simulation is equal to 44 MJ/kg and represents the energy content of the input, along with the thermal energy required by the pyrolysis reactor. In the condenser the total heat exported for cooling and condensation combined results to be 5,8 MJ/kg, while the energy content of the obtained pyrolysis oil, calculated knowing its LHV and yield, is 24,1 MJ/kg. At the end of the process, the total energy contained in the products is 21 MJ/kg, split into the 8 MJ/kg of syngas and 13 MJ/kg of carbon black. With all the data available about energy fluxes it's possible to know the conversion and total efficiencies of the plant as follows:

$$Conversion\ efficiency = \frac{Energy\ content\ of\ products}{Energy\ content\ of\ feedstock} = \frac{13MJ + 7,7MJ}{44\ MJ} = 0,47$$

The total efficiency of the process is calculated taking also into account the thermal demand:

$$Total\ efficiency = \frac{Energy\ content\ of\ products}{Total\ energy\ input} = \frac{13MJ + 7,7MJ}{44\ MJ + \ 3,7MJ\ + \ 3,8MJ} = 0,40$$

The pyrolysis oil has not been considered as a useful product because it does not satisfy the quality constraints to be burnt [69].

For what concerns the scale-up of the plant, the chosen capacity is 35 tonnes a day, which is compliant with the size of other projects of plastic pyrolysis plants in the world [70].

Lastly, in Table 9 are reported the final results of product yields with respect to the plastic feedstock mass at the inlet:

Element	Experiment final yield, wt%	Model final yield, wt%
Product gas	9 ± 1	11,2
Solid carbon	40 ± 5	39,7
Oil	52 ± 7	52,1
Hydrogen	7 ± 1	6,5
Solid residue	<0,1	0,09

Table 9 Yields of product in real life experiment and in Aspen Plus model

The yields resulting from the Aspen Plus simulation accurately replicate the results of the experiment. Another interesting point of view on the process dynamics for the understanding of the product formation processes is the comparison of the chemicals present in the

pyrolysis gas at the inlet of the thermal reactor and the syngas at the output, all reported in Table 10:

Element	Concentration in pyrolysis gas	Concentration in final syngas
CO	1,1%	1,4%
CO_2	0,7%	0 %
C_2-C_5	16%	0%
CH_4	63%	0,1%
H_2	2,8%	94,5%

Table 10 Product yields before and after thermolysis stage

The main contribution to the formation of carbon black and hydrogen is given by the C_2-C_5 hydrocarbons, that are almost completely cracked in the thermal reactor. Also methane is partially cracked, but its stronger stability at high temperatures allow to a little fraction to be present also in the final syngas. Into the thermolysis stage, it is also possible to appreciate the almost total decomposition of CO_2, helping the further formation of carbon black and CO.

The purity of hydrogen obtained in the experiment is $94,2 \pm 0,7$ %, which is a very good result if compared to the more common catalytic processes. This result has been achieved also in the Aspen Plus simulation with very good accuracy (94,5%).

5.1.2 Thermal integration and optimization

As seen in the previous section, the outcomes of the Aspen Plus simulation are compliant with the results obtained in the experiment of the reference paper [52]. The main improvement to be carried out to make feasible the scale-up is the thermal integration and optimization of the process. This point is particularly important because of the necessity of the huge temperature swings required: the pyrolysis products have to be separated into pyrolysis oil and pyrolysis gas by condensation, that reduces the temperature from 600°C to 23°C. Then the pyrolysis gas has to be thermally cracked at 1300°C and the final products to be cooled down to 130°C to guarantee the adequate operating conditions of the bag filter. On the Aspen Energy Analyzer software a simulation has been implemented in order to decrease the energy demand for both heating and cooling purposes by exploiting internally the thermal energy of the fluxes with a heat exchanger network. All the data of thermal

capacity and temperatures of the fluxes inserted in Aspen Plus Energy Analyzer have been taken from the Aspen Plus model.

Component	Heat duty (MW)
DECO + PYRO	1,22
HEATER	0,249
THERMO	1,25
Total	2,72

Table 11 Heating demand in the plant

Component	Cooling duty (MW)
COND	0,727
COOLER 1	0,987
Total	1,71

Table 12 Cooling demand in the plant

The final layout of the heat exchanger network is shown in Figure 21:
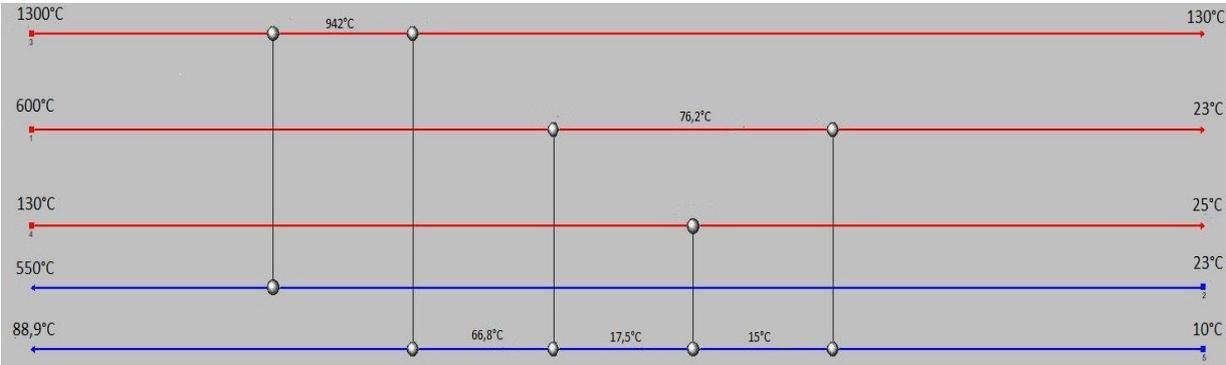
Figure 21 Aspen Energy Analyzer model of the thermal integration of the process

For what concerns the heating demand, the pre-heater of the pyrolysis gas is inserted before the thermal reactor and the increase of temperature up to 550°C is performed by putting it in contact with the outlet stream of the thermal reactor. As a consequence, the remaining cooling demand required to take the temperature of the hot products down to 130°C before entering the filters has to be satisfied with a thermal integration. Similarly, the decrease in temperature of the pyrolysis products from 600°C to 23°C and the final cooling of the syngas before entering the PSA unit need an external cooling source. The thermal integration has

been completed with a flow of 4 kg/s of cold water entering the system at a temperature of 10°C and exiting at 88,9°C. As final result, the thermal integration and optimization executed on the system led to the internal saving of 250 kW of heating demand for the thermal reactor, reducing also the operational costs required for the energy consumption, and the production of a mass flow 4 kg/s of hot water.

Considering the obtained hot water as useful product, the total efficiency of the process increases:

$$Total\ efficiency = \frac{Energy\ content\ of\ products}{Total\ energy\ input} = \frac{13MJ + 7,7MJ + 4,3\ MJ}{44\ MJ + \ 3,7MJ \ + \ 3,8MJ} = 0,48$$

where the energy content of products is the sum of the thermal energy contained in the cooling water and the chemical energy contained in the syngas and in the carbon black, while the total energy input takes into consideration the chemical energy of the plastic waste and the thermal energy required for the pyrolysis and the thermal cracking of the pyrolysis gas.

5.2 Economic analysis results

The economic analysis has been performed considering a plant lifetime of 20 years, taking as electricity price 116 €/MWh , and as gas price 32€/MWh . The considered interest rate r is equal to 2% and is assumed a debt fraction Xd of the 70% on the total initial investment.

The maintenance costs for all the components are assumed to be equal to the 2% of the component BEC every year.

Component	Total OPEX (€)
Heat exchangers	81.993
Pyrolysis reactor	448.480
Thermal reactor	1.514.622
PSA unit	3.082.476
Total	5.129.191

Table 13 Operational costs of the single components

The costs of the bag filter and the heat exchangers required is calculated with the empirical correlation, while the pyrolysis reactor, the thermal reactor and the PSA unit costs have been taken from commercial producers and literature.

Component	Cost (€)
Bag filter	9.535
Heat exchangers	103.900
Pyrolysis reactor [61]	700.000
Thermal reactor [62]	1.013.400
PSA unit [63]	1.699.833
Total	3.570.637

Table 14 Purchase cost of single components

The final TOC of the plastic thermal pyrolysis plant is 6.401.830 €

The total annual costs used to evaluate the final LCOH takes also into account the annuity and the revenues coming from the selling of carbon black, that partially helps to compensate all the operation and maintenance costs. The revenues related to carbon black are actualized to the year k and calculated considering the total annual production of the plant of 4.145.502 kg and the selling price of 1 €/kg [73]. The final LCOH calculated in the reference conditions mentioned above is of 3,76 €/kg.
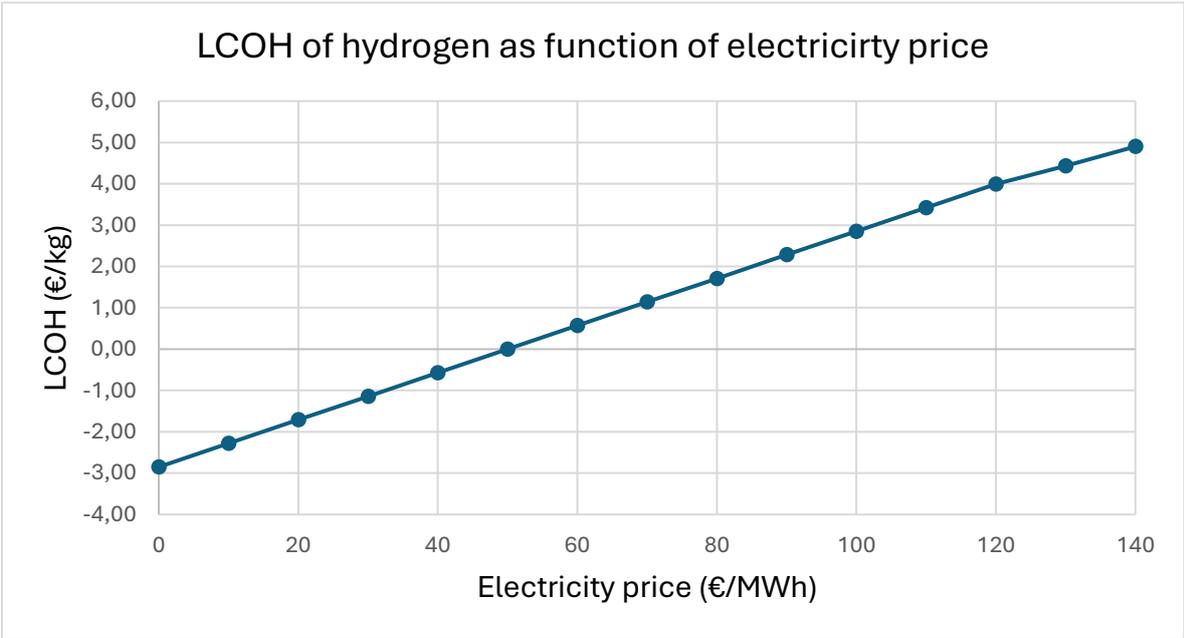

Figure 22 Effect of the variation of electricity cost on LCOH

The maximum value of the LCOH range identified in the entire study is related to the cost of electricity. For the electricity price of 140 €/MWh the LCOH increases to 4,90 €/kg. The Italian electricity market is not particularly favourable, having one of the highest electricity prices in Europe, and in the last few years even higher prices have been reached. In other European countries electricity prices below the 100 €/MWh are not so rare [74].

Notably, the LCOH goes below zero for electricity prices lower than 50 €/MWh. This is because of the contribution given by the selling of carbon black. Without it, the LCOH for 0€/MWh as electricity price would still be 3,18€/kg H_2.

5.3 Sensitivity analysis

After finding a LCOH of 3,76 €/kg, a sensitivity analysis has been performed on some of the parameters that could affect the final cost of hydrogen, in order to find the beneficial or detrimental effects deriving from their change.

Firstly, the NPV for different LCOH values has been assessed, varying the cost of hydrogen in a range of ±30% with respect to the reference value of 3,76 €/kg
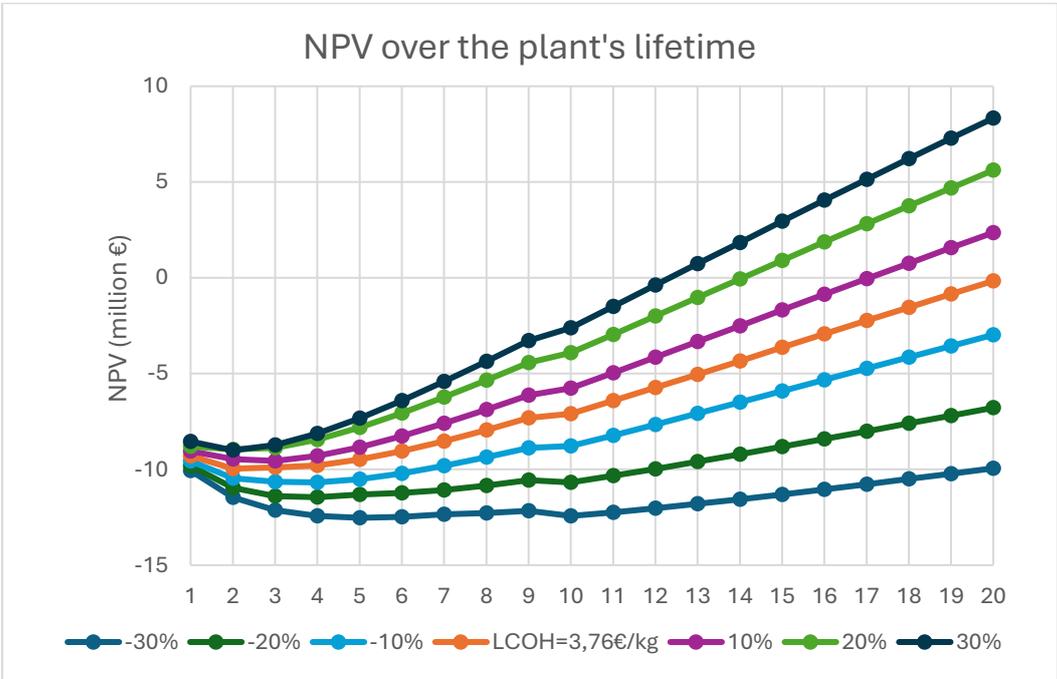

Figure 223 NPV varying the LCOH, with electricity cost 116€/kWh, gas cost 32 €/MWh and CB cost=1€/kg

At reference conditions, in the first year of life of the plant the NPV lowers its value because of the greater impact of the annuity, while in the next years the growth is more consistent and stable. At year 10 the growth is much more contained due to the extra-payments related to the pyrolysis reactor and bag filter substitutions. With the progressive increase in LCOH the initial decrease in NPV is lowered because of the increasing incomes. Moreover, the effect of the additional costs related to the substitution of the components at year 10 becomes more and more contained. On the contrary, by progressively lowering the LCOH the initial decrease in the NPV is more evident and its progressive increase over the years becomes slower.

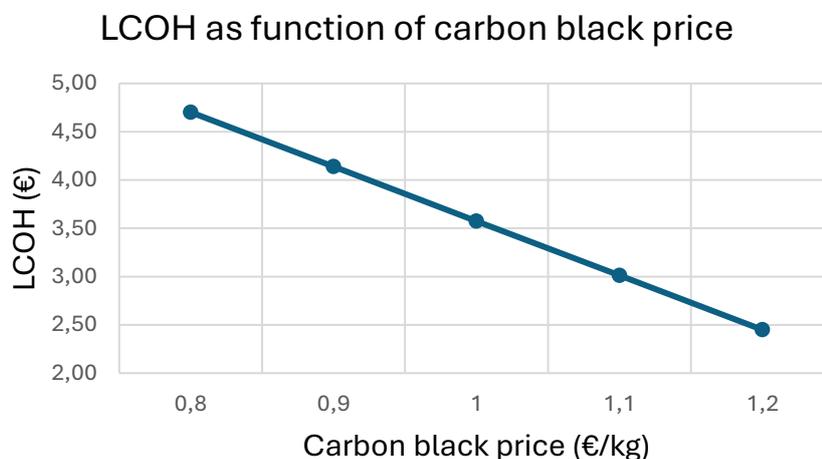The carbon black selling price is another important parameter:

Figure 23 LCOH as function of CB cost, with electricity cost 116€/kWh and gas cost 32 €/MWh

With a carbon black price ranging between 0,8-1,2 €/kg, the LCOH varies from 4,70 €/kg to 2,45 €/kg. The LCOH range is obtained setting all the other parameters with the reference values mentioned in the previous section.

In order to not only evaluate the impact strictly related to the process, like the energy price and the selling price of the co-product, also external economic factors have been assessed. The interest rate and the debt fraction on the total initial investment are the two economic parameters that change the most. The interest rate depends on external macroeconomic dynamics that are not controllable in first person by the investor. The debt fraction is referred to the amount of money that the investor puts in first person into the investment. If the investor covers the 30% of the initial investment with his own money, as firstly assumed in the reference case, the remaining 70% has to be borrowed from the outside, making the debt

fraction X_d equal to 0,7. In Figure 26 is reported the LCOH as function of the debt fraction considering all the other parameters set to reference value:

LCOH as function of debt fraction
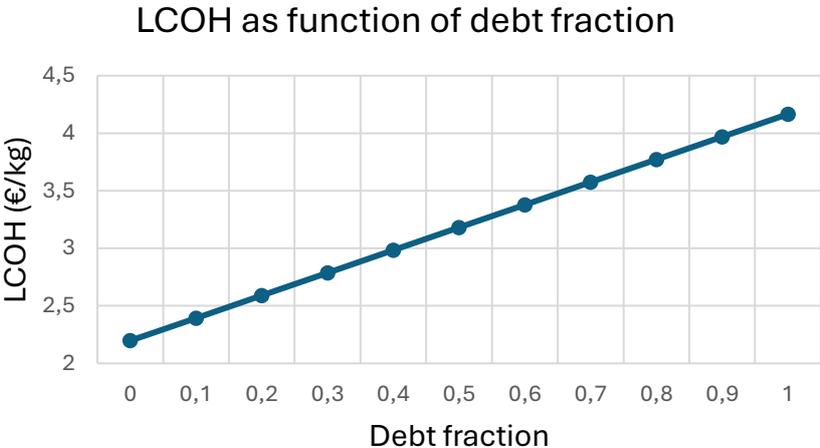
Figure 24 Influence of the debt fraction on the final LCOH, with electricity cost 116€/kWh and gas cost 32 €/MWh

With the debt fraction ranging from 0 to 1, the LCOH varies from 2,19 €/kg to 4,16 €/kg, making much more convenient for the investor to cover the larger fraction possible of the initial investment with its own money.

In Figure 26 is reported the LCOH as function of the interest rate from 1% to 4%, considering all the other parameters set to reference value:
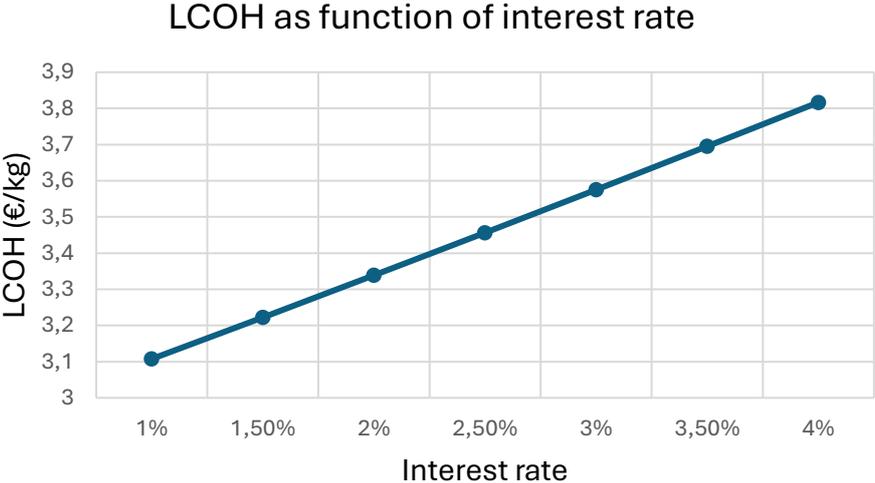
LCOH as function of interest rate

Figure 25 Effect of the interest rate on the LCOH, with electricity cost 116€/kWh and gas cost 32 €/MWh

The influence of the interest rate on the final LCOH results to be quite low if compared to all the other parameters analysed before, with the LCOH ranging from 3,10€/kg to 3,81 €/kg.

6. Conclusions

The final aim of this work was to explore the possibility of scale-up at industrial level of the co-production of carbon black and hydrogen from waste. After exploring and understanding all the current pathways for the production of these two important commodities, the plastic waste thermal pyrolysis has proved to be the most suitable process to co-produce them. Similarly to what already happens at industrial scale with the thermal cracking of light hydrocarbons, for plastic waste pyrolysis the final passage is the thermal decomposition of the resulting pyrolysis gas, obtained after the condensation of the condensable pyrolysis products into pyrolysis oil. Catalytic processes, already largely experimented in literature, have shown numerous problems related to fast catalyst deactivation and the separation of the carbon from the catalyst. In the thermal pyrolysis process these problems are automatically overcome, since there is no need of any catalyst. On the other hand, the absence of catalyst causes the requirement of very high temperatures to obtain the thermal cracking of the hydrocarbons contained in the pyrolysis gas, causing the increase of demand of thermal energy with respect to the catalytic case.

The process identified for the scale-up is directly taken from experimental literature and the scale-up itself is based in the product yields obtained in the experiment. The plastic waste identified to be the most suitable for the process is LDPE, which gives the highest hydrogen yield and the lowest amount of ashes and solid residues. With the simulation executed on Aspen Plus, all the thermal demands were calculated and the thermal integration was completed on Aspen Energy Analyser, resulting in the production of 4 kg/s of hot water at a temperature of 88,9°C. The scaled-up process has a capacity of 35 tonnes of LDPE a day, producing 686,9 tonnes per year of pure hydrogen and 4145 tonnes per year of carbon black.

The final LCOH ranges from 1,75 €/kg to 4,90€/kg, being compliant with other studies related to hydrogen production from plastic waste pyrolysis [17]. This value of LCOH is strongly dependent on electricity price and in general makes the industrial scale-up of the process to be still considered not economically convenient. As a result, there is necessity of further research and improvements to make the process suitable for the industrial applications. At the same time, it is also important to highlight that there are other technologies for hydrogen production considered to be promising for the future that

characterized by even higher costs. This makes also possible to think about the possibility of scale-up to be feasible in the near future.

7. Bibliography

[1] W. Cho, S. H. Lee, W. S. Ju, Y. Baek, and J. K. Lee, "Conversion of natural gas to hydrogen and carbon black by plasma and application of plasma carbon black," in *Catalysis Today*, Dec. 2004, pp. 633–638. doi: 10.1016/j.cattod.2004.09.051.

[2] "Origine del Carbon Black - Primax Chemical srl." Accessed: Jul. 23, 2025. [Online]. Available: https://www.primaxchemical.com/origine-del-carbon-black/

[3] "Utilizzi dell'idrogeno." Accessed: Jul. 23, 2025. [Online]. Available: https://eniscuola.eni.com/it-IT/energia/idrogeno/utilizzi-dellidrogeno.html

[4] "Applicazioni Idrogeno in Ambito Industriale - Blog - Simplifhy." Accessed: Jul. 23, 2025. [Online]. Available: https://simplifhy.com/applicazioni-presenti-e-potenziali-dellidrogeno-in-ambito-industriale/

[5] Enea, *QUADERNI DELL'EFFICIENZA ENERGETICA*.

[6] "TRL | EURAXESS." Accessed: Aug. 27, 2025. [Online]. Available: https://euraxess.ec.europa.eu/career-development/researchers/manual-scientific-entrepreneurship/major-steps/trl

[7] "Settori Applicazione Idrogeno - Decarbonizzazione Industria." Accessed: Aug. 27, 2025. [Online]. Available: https://simplifhy.com/settori/

[8] "Hydrogen production – Global Hydrogen Review 2024 – Analysis - IEA." Accessed: Aug. 29, 2025. [Online]. Available: https://www.iea.org/reports/global-hydrogen-review-2024/hydrogen-production

[9] L. Szablowski, M. Wojcik, and O. Dybinski, "Review of steam methane reforming as a method of hydrogen production," *Energy*, vol. 316, p. 134540, Feb. 2025, doi: 10.1016/J.ENERGY.2025.134540.

[10] "Hydrogen Production: Natural Gas Reforming | Department of Energy." Accessed: Aug. 28, 2025. [Online]. Available: https://www.energy.gov/eere/fuelcells/hydrogen-production-natural-gas-reforming

[11] A. Chanthakett, M. T. Arif, M. M. K. Khan, and A. M. T. Oo, "Performance assessment of gasification reactors for sustainable management of municipal solid waste," Aug. 01, 2021, *Academic Press*. doi: 10.1016/j.jenvman.2021.112661.

[12] "Chemicals from Coal Gasification, Kentucky Geological Survey, University of Kentucky." Accessed: Aug. 28, 2025. [Online]. Available: https://www.uky.edu/KGS/coal/coal-for-chemical-gasification.php

[13] S. Dermühl and U. Riedel, "A comparison of the most promising low-carbon hydrogen production technologies," *Fuel*, vol. 340, May 2023, doi: 10.1016/j.fuel.2023.127478.

[14] A. Vedrtnam, K. Kalauni, and R. Pahwa, "A review of water electrolysis technologies with insights into optimization and numerical simulations," *Int J Hydrogen Energy*, vol. 140, pp. 694–727, Jun. 2025, doi: 10.1016/J.IJHYDENE.2025.05.295.

[15] A. Ghasemi, H. Nikafshan Rad, and M. Akrami, "Biomass-to-Green Hydrogen: A Review of Techno-Economic-Enviro Assessment of Various Production Methods," *Hydrogen 2024, Vol. 5, Pages 474-493*, vol. 5, no. 3, pp. 474–493, Aug. 2024, doi: 10.3390/HYDROGEN5030027.

[16] M. Puig-Arnavat, J. C. Bruno, and A. Coronas, "Review and analysis of biomass gasification models," *Renewable and Sustainable Energy Reviews*, vol. 14, no. 9, pp. 2841–2851, Dec. 2010, doi: 10.1016/J.RSER.2010.07.030.

[17] Y. F. Khalil, "A Comparative Science-Based Viability Assessment Among Current and Emerging Hydrogen Production Technologies," *Applied Sciences 2025, Vol. 15, Page 497*, vol. 15, no. 2, p. 497, Jan. 2025, doi: 10.3390/APP15020497.

[18] "Hydrogen - FutureCoal." Accessed: Sep. 02, 2025. [Online]. Available: https://www.futurecoal.org/sustainable-coal/hydrogen/

[19] S. Hienuki, "Environmental and socio-economic analysis of naphtha reforming hydrogen energy using input-output tables: A case study from Japan," *Sustainability (Switzerland)*, vol. 9, no. 8, p. 1376, Aug. 2017, doi: 10.3390/SU9081376.

[20] "Top 10 Carbon Black Companies Worldwide in 2025 | EMR." Accessed: Sep. 13, 2025. [Online]. Available: https://www.expertmarketresearch.com/blogs/top-carbon-black-companies

[21] "Carbon Black Market Size, Share, Analysis and Forecast 2035." Accessed: Sep. 05, 2025. [Online]. Available: https://www.chemanalyst.com/industry-report/carbon-black-market-440

[22] "How is it Produced? — ICBA." Accessed: Sep. 03, 2025. [Online]. Available: https://www.carbon-black.org/is-carbon-black-safe

[23] "Oil Furnace Method Currently Used In WRPC [Asahi Carbon Limited] | Download Scientific Diagram." Accessed: Sep. 03, 2025. [Online]. Available: https://www.researchgate.net/figure/Oil-Furnace-Method-Currently-Used-In-WRPC-Asahi-Carbon-Limited_fig2_327020293

[24] C. A. Stokes and E. M. Dannenberg, "CARBON BLACKS Comparison of a Fully Reinforcing Furnace Black and Easy Processing Channel Black," UTC, 2025. [Online]. Available: https://pubs.acs.org/sharingguidelines

[25] "Comparison of Channel Carbon Black with Furnace Carbon Black and Thermal Carbon Black (Pyrolysis Carbon Black) - Beilum Carbon." Accessed: Sep. 09, 2025. [Online]. Available: https://www.beilum.com/channel-carbon-black-vs-furnace-black-thermal-black/

[26] J. Xu *et al.*, "High-value utilization of waste tires: A review with focus on modified carbon black from pyrolysis," *Science of The Total Environment*, vol. 742, p. 140235, Nov. 2020, doi: 10.1016/J.SCITOTENV.2020.140235.

[27] A. Veses *et al.*, "Pyrolysis of End-Of-Life Tires: Moving from a Pilot Prototype to a Semi-Industrial Plant Using Auger Technology," *Energy & Fuels*, vol. 38, no. 17, pp. 17087–17099, Sep. 2024, doi: 10.1021/ACS.ENERGYFUELS.4C02748.

[28] J. D. Martínez *et al.*, "Waste-based value-added feedstocks from tire pyrolysis oil distillation: defossilization of the petrochemical industry," *Green Chemistry*, vol. 27, no. 3, pp. 670–683, Jan. 2025, doi: 10.1039/D4GC05185H.

[29] "Carbon Black Prices, News, Monitor, Analysis & Demand." Accessed: Sep. 10, 2025. [Online]. Available: https://www.chemanalyst.com/Pricing-data/carbon-black-42

[30] L. Fulcheri, V. J. Rohani, E. Wyse, N. Hardman, and E. Dames, "An energy-efficient plasma methane pyrolysis process for high yields of carbon black and hydrogen," *Int J Hydrogen Energy*, vol. 48, no. 8, pp. 2920–2928, Jan. 2023, doi: 10.1016/j.ijhydene.2022.10.144.

[31] J. Diab, L. Fulcheri, V. Hessel, V. Rohani, and M. Frenklach, "Why turquoise hydrogen will Be a game changer for the energy transition," *Int J Hydrogen Energy*, vol. 47, no. 61, pp. 25831–25848, Jul. 2022, doi: 10.1016/J.IJHYDENE.2022.05.299.

[32] J. R. Fincke, R. P. Anderson, T. A. Hyde, and B. A. Detering, "Plasma pyrolysis of methane to hydrogen and carbon black," *Ind Eng Chem Res*, vol. 41, no. 6, pp. 1425–1435, Mar. 2002, doi: 10.1021/ie010722e.

[33] K. Salipira, N. J. Coville, and M. S. Scurrell, "Carbon produced by the catalytic decomposition of methane on nickel: Carbon yields and carbon structure as a function of catalyst properties," *J Nat Gas Sci Eng*, vol. 32, pp. 501–511, May 2016, doi: 10.1016/J.JNGSE.2016.04.027.

[34] G. Wang, Y. Jin, G. Liu, and Y. Li, "Production of hydrogen and nanocarbon from catalytic decomposition of methane over a Ni-Fe/Al2O3 catalyst," *Energy and Fuels*, vol. 27, no. 8, pp. 4448–4456, Aug. 2013, doi: 10.1021/EF3019707/ASSET/IMAGES/LARGE/EF-2012-019707_0012.JPEG.

[35] M. McConnachie, M. Konarova, and S. Smart, "Literature review of the catalytic pyrolysis of methane for hydrogen and carbon production," Aug. 01, 2023, *Elsevier Ltd*. doi: 10.1016/j.ijhydene.2023.03.123.

[36] A. C. Lua and H. Y. Wang, "Hydrogen production by catalytic decomposition of methane over Ni-Cu-Co alloy particles," *Appl Catal B*, vol. 156–157, pp. 84–93, Sep. 2014, doi: 10.1016/J.APCATB.2014.02.046.

[37] L. Yang, X. Wu, F. Liu, X. Zhang, J. He, and K. Saito, "Joint-use of activated carbon and carbon black to enhance catalytic stability during chemical looping methane

decomposition process," *Int J Hydrogen Energy*, vol. 45, no. 24, pp. 13245–13255, May 2020, doi: 10.1016/J.IJHYDENE.2020.03.055.

[38] B. Gaudernack and S. Lynum, "Hydrogen from natural gas without release of CO2 to the atmosphere," *Int J Hydrogen Energy*, vol. 23, no. 12, pp. 1087–1093, Dec. 1998, doi: 10.1016/S0360-3199(98)00004-4.

[39] D. Cvetinović, A. Erić, J. Anđelković, N. Ćetenović, M. Jovanović, and V. Bakić, "Economic Viability of Hydrogen Production via Plasma Thermal Degradation of Natural Gas," *Processes 2025, Vol. 13, Page 1888*, vol. 13, no. 6, p. 1888, Jun. 2025, doi: 10.3390/PR13061888.

[40] C. Wu, M. A. Nahil, N. Miskolczi, J. Huang, and P. T. Williams, "Production and application of carbon nanotubes, as a co-product of hydrogen from the pyrolysis-catalytic reforming of waste plastic," *Process Safety and Environmental Protection*, vol. 103, pp. 107–114, Sep. 2016, doi: 10.1016/J.PSEP.2016.07.001.

[41] S. S. Sharma and V. S. Batra, "Production of hydrogen and carbon nanotubes via catalytic thermo-chemical conversion of plastic waste: review," Jan. 01, 2020, *John Wiley and Sons Ltd*. doi: 10.1002/jctb.6193.

[42] C. Wu and P. T. Williams, "Pyrolysis–gasification of plastics, mixed plastics and real-world plastic waste with and without Ni–Mg–Al catalyst," *Fuel*, vol. 89, no. 10, pp. 3022–3032, Oct. 2010, doi: 10.1016/J.FUEL.2010.05.032.

[43] I. Barbarias *et al.*, "Pyrolysis and in-line catalytic steam reforming of polystyrene through a two-step reaction system," *J Anal Appl Pyrolysis*, vol. 122, pp. 502–510, Nov. 2016, doi: 10.1016/J.JAAP.2016.10.006.

[44] D. Yao *et al.*, "Co-production of hydrogen and carbon nanotubes from catalytic pyrolysis of waste plastics on Ni-Fe bimetallic catalyst," *Energy Convers Manag*, vol. 148, pp. 692–700, 2017, doi: 10.1016/j.enconman.2017.06.012.

[45] D. Yao, H. Yang, H. Chen, and P. T. Williams, "Investigation of nickel-impregnated zeolite catalysts for hydrogen/syngas production from the catalytic reforming of waste polyethylene," *Appl Catal B*, vol. 227, pp. 477–487, Jul. 2018, doi: 10.1016/J.APCATB.2018.01.050.

[46] D. Yao, Y. Zhang, P. T. Williams, H. Yang, and H. Chen, "Co-production of hydrogen and carbon nanotubes from real-world waste plastics: Influence of catalyst composition and operational parameters," *Appl Catal B*, vol. 221, pp. 584–597, 2018, doi: 10.1016/j.apcatb.2017.09.035.

[47] A. López, I. de Marco, B. M. Caballero, M. F. Laresgoiti, and A. Adrados, "Influence of time and temperature on pyrolysis of plastic wastes in a semi-batch reactor," *Chemical Engineering Journal*, vol. 173, no. 1, pp. 62–71, Sep. 2011, doi: 10.1016/J.CEJ.2011.07.037.

[48] C. Wu and P. T. Williams, "Pyrolysis–gasification of post-consumer municipal solid plastic waste for hydrogen production," *Int J Hydrogen Energy*, vol. 35, no. 3, pp. 949–957, Feb. 2010, doi: 10.1016/J.IJHYDENE.2009.11.045.

[49] G. Bajad, R. P. Vijayakumar, P. Rakhunde, A. Hete, and M. Bhade, "Processing of mixed-plastic waste to fuel oil, carbon nanotubes and hydrogen using multi–core reactor," *Chemical Engineering and Processing: Process Intensification*, vol. 121, pp. 205–214, Nov. 2017, doi: 10.1016/J.CEP.2017.09.011.

[50] I. Barbarias, G. Lopez, M. Artetxe, A. Arregi, J. Bilbao, and M. Olazar, "Valorisation of different waste plastics by pyrolysis and in-line catalytic steam reforming for hydrogen production," *Energy Convers Manag*, vol. 156, pp. 575–584, Jan. 2018, doi: 10.1016/J.ENCONMAN.2017.11.048.

[51] I. Barbarias *et al.*, "A sequential process for hydrogen production based on continuous HDPE fast pyrolysis and in-line steam reforming," *Chemical Engineering Journal*, vol. 296, pp. 191–198, Jul. 2016, doi: 10.1016/J.CEJ.2016.03.091.

[52] A. Veksha, Y. Wang, J. W. Foo, I. Naruse, and G. Lisak, "Defossilization and decarbonization of hydrogen production using plastic waste: Temperature and feedstock effects during thermolysis stage," *J Hazard Mater*, vol. 452, Jun. 2023, doi: 10.1016/j.jhazmat.2023.131270.

[53] R. K. Singh, B. Ruj, A. K. Sadhukhan, and P. Gupta, "Thermal degradation of waste plastics under non-sweeping atmosphere: Part 1: Effect of temperature, product optimization, and degradation mechanism," *J Environ Manage*, vol. 239, pp. 395–406, Jun. 2019, doi: 10.1016/J.JENVMAN.2019.03.067.

[54] N. Muradov, "Hydrogen via methane decomposition: an application for decarbonization of fossil fuels," *Int J Hydrogen Energy*, vol. 26, no. 11, pp. 1165–1175, Nov. 2001, doi: 10.1016/S0360-3199(01)00073-8.

[55] "Choosing the Best Materials for Bag Filters in Boilers. - Steamaxindia." Accessed: Oct. 23, 2025. [Online]. Available: https://steamaxindia.com/choosing-the-best-materials-for-bag-filters-in-boilers/

[56] "The Working Principle of Pressure Swing Adsorption (PSA)." Accessed: Oct. 27, 2025. [Online]. Available: https://absstem.com/the-working-principle-of-pressure-swing-adsorption-psa/

[57] H. J. K. Shabbani, M. R. Othman, S. K. Al-Janabi, A. R. Barron, and Z. Helwani, "H2 purification employing pressure swing adsorption process: Parametric and bibliometric review," *Int J Hydrogen Energy*, vol. 50, pp. 674–699, Jan. 2024, doi: 10.1016/J.IJHYDENE.2023.11.069.

[58] "QUALITY GUIDELINES FOR ENERGY SYSTEM STUDIES Cost Estimation Methodology for NETL Assessments of Power Plant Performance," 2021. [Online]. Available: www.netl.doe.gov

[59] "Analysis, Synthesis, and Design of Chemical Processes, Fifth Edition."

[60] "2025 CEPCI updates: July (prelim.) and June (final) - Chemical Engineering." Accessed: Oct. 28, 2025. [Online]. Available: https://www.chemengonline.com/2025-cepci-updates-july-prelim-and-june-final/?printmode=1

[61] "Pyrolysis Plant Cost - Get Reasonable Price from Beston Group." Accessed: Oct. 17, 2025. [Online]. Available: https://www.bestongroup.com/pyrolysis-plant/cost/

[62] "PRODUCT OVERVIEW FIBROTHAL™ HEATING MODULES AND INSULATION SYSTEMS 2 HEATING MODULES AND INSULATION SYSTEMS HEATING MODULES AND INSULATION SYSTEMS 3 CONTENT Introduction 4."

[63] I. Burgers, L. Dehdari, P. Xiao, K. G. Li, E. Goetheer, and P. Webley, "Techno-economic analysis of PSA separation for hydrogen/natural gas mixtures at hydrogen

refuelling stations," *Int J Hydrogen Energy*, vol. 47, no. 85, pp. 36163–36174, Oct. 2022, doi: 10.1016/j.ijhydene.2022.08.175.

[64]   C. Jackson, G. Smith, and A. R. Kucernak, "Deblending and purification of hydrogen from natural gas mixtures using the electrochemical hydrogen pump," *Int J Hydrogen Energy*, vol. 52, pp. 816–826, Jan. 2024, doi: 10.1016/j.ijhydene.2023.05.065.

[65]   "EU Natural Gas TTF - Price - Chart - Historical Data - News." Accessed: Oct. 28, 2025. [Online]. Available: https://tradingeconomics.com/commodity/eu-natural-gas

[66]   "Prezzo dell'elettricità in Italia | 2004-2025 Dati | 2026-2027 Previsione." Accessed: Oct. 28, 2025. [Online]. Available: https://it.tradingeconomics.com/italy/electricity-price

[67]   "Tariffa del Servizio Idrico Integrato - SMAT." Accessed: Oct. 28, 2025. [Online]. Available: https://www.smatorino.it/tariffa-del-servizio-idrico-integrato-2/

[68]   Y. Shen, "Microwave-assisted Pyrolysis of Biomass and Plastic Wastes for Hydrogen Production," *Green Chemistry*, 2025, doi: 10.1039/d5gc03030g.

[69]   Z. Chen, W. Wei, X. Chen, Y. Liu, Y. Shen, and B. J. Ni, "Upcycling of plastic wastes for hydrogen production: Advances and perspectives," *Renewable and Sustainable Energy Reviews*, vol. 195, p. 114333, May 2024, doi: 10.1016/J.RSER.2024.114333.

[70]   F. Niu *et al.*, "State-of-the-art and perspectives of hydrogen generation from waste plastics," Apr. 15, 2025, *Royal Society of Chemistry*. doi: 10.1039/d4cs00604f.

[71]   E. Giglio, M. Bianco, G. Zanardi, E. Catizzone, G. Giordano, and M. Migliori, "Direct biogas methanation via renewable-based Power-to-Gas: Techno-economic assessment based on real industrial data," *Energy Convers Manag*, vol. 332, May 2025, doi: 10.1016/j.enconman.2025.119775.

[73]   "Carbon Black Prices, Trends, Index, News, Monitor and Demand." Accessed: Oct. 28, 2025. [Online]. Available: https://www.chemanalyst.com/Pricing-data/carbon-black-42

[74]   "⚡ Electricity prices Europe." Accessed: Oct. 30, 2025. [Online]. Available: https://euenergy.live/